# Multiple single-photon generations in three-level atoms coupled to a cavity with non-Markovian effects

H. Z. Shen,[1,2,*] Y. Chen,[1] T. Z. Luan,[1] and X. X. Yi[1,2,†]

[1]*Center for Quantum Sciences and School of Physics, Northeast Normal University, Changchun 130024, China*

[2]*Center for Advanced Optoelectronic Functional Materials Research and Key Laboratory for UV Light-Emitting Materials and Technology of Ministry of Education, Northeast Normal University, Changchun 130024, China*

(Received 16 June 2022; revised 19 March 2023; accepted 26 April 2023; published 8 May 2023)

In this paper we show how to generate multiple single-photon wave packets of arbitrary temporal shape from an optical cavity coupled with $N$ three-level atoms driven by a driving field in the non-Markovian regime. We derive an exact analytical expression of the optimal driving field to generate such wave packets, which depends on two detunings of the cavity and driving field with respect to the three-level atoms. The cavity we use consists of two mirrors facing each other, where one is perfect and the other includes dissipation (a one-sided cavity), which couples with the corresponding non-Markovian input-output fields. If the first single-photon wave packet generated by the Markovian system is the same as the non-Markovian case, the Markovian system cannot generate the same multiple single-photon wave packets as the non-Markovian system when the spectral widths of the other environments take values different from the spectral width of the first environment, while setting the equal spectral widths for the different environments can generate this. The generated multiple different single-photon wave packets are not independent of each other, which satisfies certain relations with non-Markovian spectral parameters. We analyze the transition from Markovian to non-Markovian regimes and compare the differences between them, where the cavity interacts simultaneously with the multiple non-Markovian environments. Finally, we extend the above results to a general non-Markovian quantum network involving many cavities coupled with driven three-level atoms.

DOI: 10.1103/PhysRevA.107.053705

## I. INTRODUCTION

Quantum networks composed of local nodes, which are connected by quantum channels, are essential for quantum communication and desirable for scalable and distributed quantum computation [1–12]. The stationary qubits in local nodes can be provided by collective atomic excitations [13–15]. A photon wave packet is an ideal carrier for a flying qubit, with either the photon-number states or the polarization forming the qubit. The controlled production of single photons [16,17] is of fundamental and practical interest, which denotes the lowest excited quantum states of the radiation field, and has applications in quantum information processing [18]. The single-photon generation [19–22] by a coupled atom cavity [23–39] system has been demonstrated in the Markovian case. After that, several similar schemes were put forward [40–61]. The prototype quantum interface for this purpose was proposed by Yao *et al.* [62], where the presented Raman process can be made to generate or annihilate [62–66] an arbitrarily shaped single-photon wave packet by pulse shaping the controlling laser field.

Markovian processes successfully describe many physical phenomena, especially in the field of quantum optics, but they fail when they are applied to more complex system-environment couplings, where memory effects play the dominating roles. Generally speaking, all realistic quantum systems are open due to the unavoidable couplings to environment (of memory or memoryless) [67–70]. Considering the non-Markovian [71–106] dynamics of open quantum systems is essential in quantum information technology. In particular, a notion of memory for quantum processes has been introduced, which can be physically interpreted in terms of information flow between the open system and its environments. So far, several scenarios have been recognized under which the non-Markovian dynamics can happen, for example, strong system-environment coupling, structured reservoirs, low temperatures, and initial system-environment correlations [107–115]. Generally, people focus on the quantum system coupled to a single environment, which has been investigated theoretically [116–126] and experimentally [127–134]. However, in the real world, there might be a situation of many environments coupling to a system simultaneously [82,135–146].

The above two considerations motivate us to explore the generations of multiple complex single-photon wave packets from an optical cavity coupled to the driven three-level atoms with non-Markovian input-output fields.

In this paper we present a scheme of generating the multiple complex single-photon wave packets from the cavity coupled with $N$ driven three-level atoms in the non-Markovian regime. To generate such wave packets, we derive an analytical solution of the optimal driving field, which is affected

*Corresponding author: shenhz458@nenu.edu.cn

†Corresponding author: yixx@nenu.edu.cn

 

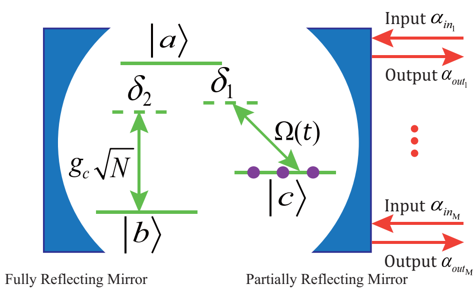


FIG. 1. Multiple complex single-photon generations in three-level atoms coupled to a cavity with non-Markovian effects. The system is composed of a one-sided cavity coupled to $N$ three-level $\Lambda$ atoms, where the cavity interacts simultaneously with $M$ non-Markovian input-output fields. Every atom has three levels, i.e., the ground-state hyperfine levels $|b\rangle$ and $|c\rangle$ [152,153], and the excited state $|a\rangle$. Three-level atoms interact with the cavity and are driven by a classical field with the coupling strength $g_c\sqrt{N}$ and driving field $\Omega(t)$. The purple circles denote schematically that the atomic population is concentrated in the state $|c\rangle$. The classical field and cavity are detuned from the atoms denoted by $\delta_1$ and $\delta_2$, respectively.

by two detunings of the cavity and driving field with respect to the three-level atoms. When the first single-photon wave packets generated by the Markovian and non-Markovian systems are equal, the same multiple single-photon wave packets in the non-Markovian regime cannot be generated by a Markovian system if all the other spectral widths do not equal the first one, while setting the equal spectral widths for the different environments can generate this. Moreover, we study the non-Markovian dynamics of generating the multiple output single-photon wave packets from one side of the cavity coupled simultaneously with multiple identical and different non-Markovian input-output fields, for which certain correlations related to non-Markovian spectral parameters exist. Finally, the above results are extended to a non-Markovian input-output quantum network consisting of many cavities containing driven three-level atoms.

Our paper is outlined as follows. In Sec. II we illustrate a model to describe the driven three-level atoms coupled to a cavity, which interacts simultaneously with multiple non-Markovian input-output fields. In Sec. III we present the exact solutions of the optimal driving field for generating the multiple single-photon wave packets. In Sec. IV we compare the cases of a single-photon generation with and without the Markovian approximations. In Sec. V we study the multiple single-photon generations, where the cavity simultaneously interacts with the multiple non-Markovian input-output fields by taking the equal and nonequal values for the spectral widths of the different environments in the Markovian and non-Markovian systems. Section VI is devoted to a discussion of the non-Markovian quantum input-output network with many driven atom-cavity systems. In Sec. VII we summarize the paper.

## II. MODEL AND EXACT NON-MARKOVIAN DYNAMICS

The proposed scheme for the non-Markovian multiple complex single-photon generations is depicted in Fig. 1, where a Fabry-Pérot cavity couples to $N$ identical three-level $\Lambda$-type atoms in the basis of collective states. We now discuss how to generate the shapes of the specified single-photon wave packets if there are no incoming photons. The single-photon pulse shapes, provided they are smooth enough, can be arbitrarily specified. The total system is described by the Hamiltonian $\hat{H} = \hat{H}_S + \hat{H}_B + \hat{V}$ in the rotating frame (setting $\hbar \equiv 1$)

$$\hat{H}_S = \sum_{m=1}^{N} \{[\Omega(t)e^{i\delta_1 t}\hat{\sigma}_{ac}^{(m)} + g_c\hat{\sigma}_{ab}^{(m)}\hat{a}e^{i\delta_2 t} + \text{H.c.}] - i\gamma'\hat{\sigma}_{aa}^{(m)}\},$$

$$\hat{H}_B = \sum_{j=1}^{M} \int d\omega_j \Omega_{\omega_j} \hat{b}_j^\dagger(\omega_j)\hat{b}_j(\omega_j),$$

$$\hat{V} = i\sum_{j=1}^{M} \int d\omega_j [v_j(\omega_j)\hat{a}\hat{b}_j^\dagger(\omega_j) - \text{H.c.}], \tag{1}$$

where $\hat{\sigma}_{\mu,\nu}^{(m)} = |\mu\rangle_{mm}\langle\nu|$ $(\mu, \nu = a, b, c)$ is the flip operator of the $m$th atom between states $|\mu\rangle$ and $\langle\nu|$, H.c. stands for the Hermitian conjugate, $\hat{b}_j(\omega_j)$ $[\hat{b}_j^\dagger(\omega_j)]$ is the annihilation (creation) operator for the frequency $\omega_j$ in the $j$th continuum field (it can also be called the $j$th environment), and $\hat{a}$ $(\hat{a}^\dagger)$ denotes the annihilation (creation) operator of the cavity. The interaction between the cavity and continuum field is described by the Hamiltonian $\hat{V}$ with the strength $v_j(\omega_j)$ [68,72,147,148], where $[\hat{b}_j(\omega_j), \hat{b}_j^\dagger(\omega_j')] = \delta(\omega_j - \omega_j')$ and $[\hat{a}, \hat{a}^\dagger] = 1$. The derivation of Eq. (1) can be found in Appendix A. In view of the symmetry of the couplings, it is convenient to introduce collective atomic operators $\tilde{\sigma}_{ab} = \sum_{m=1}^{N}\hat{\sigma}_{ab}^{(m)}$, $\tilde{\sigma}_{ac} = \sum_{m=1}^{N}\hat{\sigma}_{ac}^{(m)}$, and $\tilde{\sigma}_{aa} = \sum_{m=1}^{N}\hat{\sigma}_{aa}^{(m)}$. When all atoms are prepared initially in level $|b\rangle$, the only states coupled by the interaction are totally symmetric Dicke-like states [149,150]

$$|b\rangle \equiv |b_1 \cdots b_m \cdots b_N\rangle,$$

$$|a\rangle \equiv \frac{1}{\sqrt{N}}\sum_{m=1}^{N}\left|a_m \prod_{\otimes k=1}^{N} b_{k\neq m}\right\rangle,$$

$$|c\rangle \equiv \frac{1}{\sqrt{N}}\sum_{m=1}^{N}\left|c_m \prod_{\otimes k=1}^{N} b_{k\neq m}\right\rangle, \tag{2}$$

where the introduced factor $1/\sqrt{N}$ in front of Eq. (2) meets the state normalization requirements, i.e., $\langle a|a\rangle = \langle c|c\rangle = 1$. The $|b\rangle \to |a\rangle$ transition is coupled to the cavity with the strength $g_c$, which is assumed to be equal for all atoms. The detuning $\delta_2$ is defined as $\delta_2 = \omega_a - \omega_b - \omega_{\text{cav}}$ ($\omega_{\text{cav}}$ is the center frequency of the cavity). The $|c\rangle \to |a\rangle$ transition is coupled by the time-dependent driving field $\Omega(t)$ (i.e., the Rabi frequency of the driving field) [151] with the detuning $\delta_1 = \omega_a - \omega_c - \omega_L$, where $\omega_L$ is the frequency of the classical field;$\omega_b$, $\omega_c$, and $\omega_a$ denote the eigenfrequencies of states $|b\rangle$, $|c\rangle$, and $|a\rangle$, respectively; $\gamma'$ is the atomic spontaneous emission rate; and $\Omega_{\omega_j} = \omega_j - \omega_{\text{cav}}$ denotes the detuning of the $\omega_j$ mode of the continuum fields from the center frequency of the cavity.

The atom-cavity interacts with input-output fields by bases $|b, 1, 0\rangle$, $|c, 0, 0\rangle$, $|a, 0, 0\rangle$, and $|b, 0, 1_{\omega_j}\rangle$, respectively, where $|s, n, 0\rangle = |s\rangle \otimes |n\rangle \otimes |0\rangle$ and $|s, n, 1_{\omega_j}\rangle = |s\rangle \otimes |n\rangle \otimes |1_{\omega_j}\rangle$ ($s = a, b, c$, and $n$ is the number of photons in the cavity), $|0\rangle = |\cdots 0_1, 0_2, \cdots 0_M \cdots\rangle$ corresponds to the continuum fields at its vacuum state, and $|1_{\omega_j}\rangle = |\cdots 0_1, 0_2, \cdots 1_{\omega_j} \cdots 0_M \cdots\rangle$ denotes the one-photon Fock state of the continuum fields with frequency $\omega_j$. The state of the total system can be expressed in the compact form

$$|\Psi(t)\rangle = \beta_b(t)|b, 1, 0\rangle + \beta_c(t)|c, 0, 0\rangle + \beta_a(t)|a, 0, 0\rangle + \sum_{j=1}^{M} \int d\omega_j \alpha_{\omega_j}(t)|b, 0, 1_{\omega_j}\rangle. \quad (3)$$

With these relations $\tilde{\sigma}_{ba}|a\rangle = \sqrt{N}|b\rangle$, $\tilde{\sigma}_{ab}|b\rangle = \sqrt{N}|a\rangle$, $\tilde{\sigma}_{ca}|a\rangle = |c\rangle$, and $\tilde{\sigma}_{ac}|c\rangle = |a\rangle$, substituting Eqs. (1) and (3) into Schrödinger equation $i|\dot{\Psi}(t)\rangle = \hat{H}|\Psi(t)\rangle$, we obtain a set of the differential equations for the probability amplitudes

$$\dot{\beta}_b(t) = -ig_c\sqrt{N}e^{-i\delta_2 t}\beta_a(t) - \sum_{j=1}^{M}\int_{-\infty}^{+\infty} d\omega_j v_j^*(\omega_j)\alpha_{\omega j}(t), \quad (4)$$

$$\dot{\beta}_c(t) = -i\Omega^*(t)e^{-i\delta_1 t}\beta_a(t), \quad (5)$$

$$\dot{\beta}_a(t) = -ig_c\sqrt{N}e^{i\delta_2 t}\beta_b(t) - i\Omega(t)e^{i\delta_1 t}\beta_c(t) - \gamma'\beta_a(t), \quad (6)$$

$$\dot{\alpha}_{\omega_j}(t) = -i\Omega_{\omega_j}\alpha_{\omega_j}(t) + v_j(\omega_j)\beta_b(t). \quad (7)$$

Integrating Eq. (7), we obtain

$$\alpha_{\omega_j}(t) = e^{-i\Omega_{\omega_j}t}\alpha_{\omega_j}(0) + v_j(\omega_j)\int_0^t d\tau\, \beta_b(\tau)e^{-i\Omega_{\omega_j}(t-\tau)} \quad (8)$$

or

$$\alpha_{\omega_j}(t) = e^{-i\Omega_{\omega_j}(t-t_1)}\alpha_{\omega_j}(t_1) - v_j(\omega_j)\int_t^{t_1} d\tau\, \beta_b(\tau)e^{-i\Omega_{\omega_j}(t-\tau)}, \quad (9)$$

where $t_1 \geqslant t$. Substituting Eq. (8) into Eq. (4), we get the non-Markovian integro-differential equations for the probability amplitudes

$$\begin{aligned}\dot{\beta}_b(t) &= -ig_c\sqrt{N}e^{-i\delta_2 t}\beta_a(t) - \sum_{j=1}^{M}\int_0^t d\tau\, F_j(t-\tau)\beta_b(\tau) + \sum_{j=1}^{M}\int d\tau\, k_j^*(\tau - t)\alpha_{in_j}(\tau),\\ \dot{\beta}_c(t) &= -i\Omega^*(t)e^{-i\delta_1 t}\beta_a(t),\\ \dot{\beta}_a(t) &= -ig_c\sqrt{N}e^{i\delta_2 t}\beta_b(t) - \gamma'\beta_a(t) - i\Omega(t)e^{i\delta_1 t}\beta_c(t).\end{aligned} \quad (10)$$

The input fields $\alpha_{\mathrm{in}_j}(t)$ in the non-Markovian regime related to the output fields $\alpha_{\mathrm{out}_j}(t)$ by the multiple input-output relations are derived as

$$\alpha_{\mathrm{in}_j}(t) + \alpha_{\mathrm{out}_j}(t) = \int_0^t d\tau\, k_j(t-\tau)\beta_b(\tau), \quad (11)$$

where

$$\alpha_{\mathrm{in}_j}(t) = -\frac{1}{\sqrt{2\pi}}\int_{-\infty}^{+\infty} d\omega_j \alpha_{\omega_j}(0)e^{-i\Omega_{\omega_j}t} \quad (12)$$

and

$$\alpha_{\mathrm{out}_j}(t) = \frac{1}{\sqrt{2\pi}}\int_{-\infty}^{+\infty} d\omega_j \alpha_{\omega_j}(t_1)e^{-i\Omega_{\omega_j}(t-t_1)}. \quad (13)$$

The details of the derivation in Eqs. (10) and (11) can be found in Appendixes B and C, respectively. The response function and correlation function can be written as

$$k_j(t) = \frac{1}{\sqrt{2\pi}}\int_{-\infty}^{\infty} d\omega_j e^{-i\Omega_{\omega_j}t}v_j(\omega_j) \quad (14)$$

and

$$F_j(t-\tau) = \int_{-\infty}^{+\infty} d\omega_j J_j(\omega_j)e^{-i\Omega_{\omega_j}(t-\tau)}, \quad (15)$$

respectively, where $J_j(\omega_j) = |v_j(\omega_j)|^2$ represents the spectral density. We assume $v_j(\omega_j) = \lambda_j\sqrt{\gamma_j/2\pi}/[\lambda_j - i(\omega_j - \omega_{\mathrm{cav}})]$ and

$$J_j(\omega_j) = \frac{\gamma_j}{2\pi}\frac{\lambda_j^2}{\lambda_j^2 + (\omega_j - \omega_{\mathrm{cav}})^2}, \quad (16)$$

where $\gamma_j$ and $\lambda_j$ denote the decay rate and spectral width of the $j$th environment, respectively. In the non-Markovian regime, we have $k_j(t) = \lambda_j\sqrt{\gamma_j}u(t)e^{-\lambda_j t}$ and $F_j(t) = \frac{1}{2}\lambda_j\gamma_j e^{-\lambda_j|t|}$, where $u(t)$ is the unit step function, i.e., $u(t) = 1$ for $t \geqslant 0$ and otherwise $u(t) = 0$. Under the Markovian approximation, the spectral density $J_j(\omega_j) \to \gamma_j/2\pi$ and coupling strength $v_j(\omega_j) \to \sqrt{\gamma_j/2\pi}$ lead to

$$k_j(t) = \sqrt{\gamma_j}\delta(t), \quad F_j(t) = \gamma_j\delta(t). \quad (17)$$

Substituting Eq. (17) into Eqs. (10) and (11), we obtain

$$\begin{aligned}\dot{\beta}_b(t) &= -ig_c\sqrt{N}e^{-i\delta_2 t}\beta_a(t) + \sum_{j=1}^{M}\sqrt{\gamma_j}\alpha_{\mathrm{in}_j}(t) - \sum_{j=1}^{M}\tfrac{1}{2}\gamma_j\beta_b(t),\\ \dot{\beta}_c(t) &= -i\Omega^*(t)e^{-i\delta_1 t}\beta_a(t),\\ \dot{\beta}_a(t) &= -ig_c\sqrt{N}e^{i\delta_2 t}\beta_b(t) - \gamma'\beta_a(t) - i\Omega(t)e^{i\delta_1 t}\beta_c(t),\\ \alpha_{\mathrm{in}_j}(t) &+ \alpha_{\mathrm{out}_j}(t) = \sqrt{\gamma_j}\beta_b(t).\end{aligned} \quad (18)$$

We show that from Eq. (10) the probability amplitudes and driving field are expressed in terms of $\alpha_{\mathrm{in}_j}(t)$ and $\alpha_{\mathrm{out}_j}(t)$, which can be arbitrarily specified and generated on demand by meeting the normalization condition of Eq. (3).

## III. NON-MARKOVIAN MULTIPLE SINGLE-PHOTON GENERATIONS AND OPTIMAL DRIVING FIELD

In the following we discuss in more detail that the system can generate the multiple complex single-photon wave packets. If initially the three-level system is entirely in state

$|c, 0, 0\rangle$, this mapping operation can function as the deterministic generation of the single-photon wave packets with any desired pulse shape $\alpha_{\text{out}_j}(t)$. The initial conditions for the above scheme take $\alpha_{\text{in}_j}(t) = 0$, $\beta_b(0) = 0$, $\beta_c(0) = 1$, and $\beta_a(0) = 0$, together with Eqs. (10) and (11), which lead to

$$\beta_b(t) = \frac{\dot{\alpha}_{\text{out}_j}(t) + \lambda_j \alpha_{\text{out}_j}(t)}{\lambda_j \sqrt{\gamma_j}}, \tag{19}$$

$$\tilde{\beta}_a(t) = \frac{-\dot{\beta}_b(t) - \sum_{j=1}^{M} \int_0^t d\tau\, F_j(t-\tau)\beta_b(\tau)}{g_c\sqrt{N}}, \tag{20}$$

where we have defined $\tilde{\beta}_a(t) = ie^{-i\delta_2 t}\beta_a(t)$. In order not to lose generality, we assume that the target pulse shapes of the output single-photon wave packets are specified to be complex functions in time with the interaction picture so that $\beta_b(t)$ and $\tilde{\beta}_a(t)$ are also complex functions in this case. According to Eq. (10), we get

$$\Omega(t)\tilde{\beta}_c(t) = \dot{\tilde{\beta}}_a(t) + i\delta_2\tilde{\beta}_a(t) - g_c\sqrt{N}\beta_b(t) + \gamma'\tilde{\beta}_a(t), \tag{21}$$

$$\Omega^*(t)\tilde{\beta}_a(t) = -i\tilde{\delta}\tilde{\beta}_c(t) - \dot{\tilde{\beta}}_c(t), \tag{22}$$

where $\tilde{\beta}_c(t) = e^{-i\tilde{\delta}t}\beta_c(t)$ and $\tilde{\delta} = \delta_2 - \delta_1$. Based on Eqs. (21) and (22), we obtain the population of the atom in the state $|c\rangle$ with non-Markovian effects

$$\rho_c(t) = 1 - |\tilde{\beta}_a(t)|^2 + \int_0^t dt'\{2g_c\sqrt{N}\text{Re}[\tilde{\beta}_a(t')\beta_b^*(t')] - 2\gamma'|\tilde{\beta}_a(t')|^2\}, \tag{23}$$

where $\rho_c(t) = |\tilde{\beta}_c(t)|^2$, which does not depend on the detunings $\delta_1$ and $\delta_2$. The strategy is to design the driving field $\Omega(t)$ from Eqs. (21) and (22) as

$$\Omega(t) = \chi(t)[\dot{\tilde{\beta}}_a(t) + i\delta_2\tilde{\beta}_a(t) - g_c\sqrt{N}\beta_b(t) + \gamma'\tilde{\beta}_a(t)] \tag{24}$$

to generate the multiple single-photon wave packets with non-Markovian effects, where $\chi(t) = \exp\int_0^t dt'\{[i\tilde{\delta}\rho_c(t') + \tilde{\beta}_a(t')\dot{\tilde{\beta}}_a^*(t') - i\delta_2|\tilde{\beta}_a(t')|^2 - g_c\sqrt{N}\tilde{\beta}_a(t')\beta_b^*(t') + \gamma'|\tilde{\beta}_a(t')|^2] /\rho_c(t')\}$. In this case, we find that the optimal driving field $\Omega(t)$ depends on two detunings $\delta_1$ and $\delta_2$ for the generations of the multiple complex single-photon wave packets (it will be exhibited at the ending of Sec. IV), which completely differs from the previous proposals [6–8,49–51,62–66].

In particular, assuming that the output single-photon wave packets are real functions with the time in the interaction picture so that $\beta_b(t)$ and $\tilde{\beta}_a(t)$ also are real ones, we obtain the exact analytical expression for the optimal driving field to generate the desired output single-photon wave packets as $\Omega(t) = P(t) + iQ(t)$, whose argument and modulus are expressed by

$$\arg[\Omega(t)] = \arctan\left(\frac{Q(t)}{P(t)}\right), \tag{25}$$

$$|\Omega(t)| = \sqrt{\frac{[\dot{\tilde{\beta}}_a(t) - g_c\sqrt{N}\beta_b(t) + \gamma'\tilde{\beta}_a(t)]^2 + \delta_2^2\tilde{\beta}_a^2(t)}{\rho_c(t)}}, \tag{26}$$

respectively, where $P(t) = [\dot{\tilde{\beta}}_a(t)\cos\alpha(t) - g_c\sqrt{N}\beta_b(t) \cos\alpha(t) + \gamma'\tilde{\beta}_a(t)\cos\alpha(t) + \delta_2\tilde{\beta}_a(t)\sin\alpha(t)]/\sqrt{\rho_c(t)}$ and $Q(t) = [\delta_2\tilde{\beta}_a(t)\cos\alpha(t) + g_c\sqrt{N}\beta_b(t)\sin\alpha(t) - \dot{\tilde{\beta}}_a(t)\sin\alpha(t) - \gamma'\tilde{\beta}_a(t)\sin\alpha(t)]/\sqrt{\rho_c(t)}$, with $\alpha(t) = -\tilde{\delta}t + \delta_2\int_0^t \tilde{\beta}_a^2(t')/ \rho_c(t')dt'$. Equations (25) and (26) tell us that the modulus of the optimal driving field $\Omega(t)$ only has a bearing on the detuning $\delta_2$, while the detunings $\delta_1$ and $\delta_2$ produce the influences on the argument $\arg[\Omega(t)]$. Based on this, we show that the scheme under study for any given multiple single-photon wave packets requires the driving field depending on two detunings (i.e., the detunings $\delta_1$ and $\delta_2$ of the cavity and driving field with respect to the three-level atoms) and non-Markovian effects, which completely differs from those of three-level system shown in Refs. [6–8,49–51,62–66], where these schemes mainly focused on the resonance case ($\delta_1 = \delta_2 \equiv 0$) and Markovian approximation. Under the Markovian approximation with Eq. (18) (we denote the quantities in the Markovian case by introducing a subscript $f$ to them), subjected to the initial conditions $\alpha_{\text{in}_j}(t) = 0$, $\beta_{bf}(0) = 0$, $\beta_{cf}(0) = 1$, and $\beta_{af}(0) = 0$, we can obtain

$$\beta_{bf}(t) = \frac{\alpha_{\text{out}_{jf}}(t)}{\sqrt{\gamma_j}}, \quad \tilde{\beta}_{af}(t) = \frac{-\dot{\beta}_{bf}(t) - \sum_{j=1}^{M}\frac{1}{2}\gamma_j\beta_{bf}(\tau)}{g_c\sqrt{N}},$$
$$\rho_{cf}(t) = 1 - |\tilde{\beta}_{af}(t)|^2 + \int_0^t dt'\{2g_c\sqrt{N}\text{Re}[\tilde{\beta}_{af}(t')\beta_{bf}^*(t')] - 2\gamma'|\tilde{\beta}_{af}(t')|^2\},$$
$$\Omega_f(t) = P_f(t) + iQ_f(t), \tag{27}$$

with

$$P_f(t) = [\dot{\tilde{\beta}}_{af}(t)\cos\alpha_f(t) - g_c\sqrt{N}\beta_{bf}(t)\cos\alpha_f(t) + \gamma'\tilde{\beta}_{af}(t)\cos\alpha_f(t) + \delta_2\tilde{\beta}_{af}(t)\sin\alpha_f(t)]/\sqrt{\rho_{cf}(t)},$$
$$Q_f(t) = [\delta_2\tilde{\beta}_{af}(t)\cos\alpha_f(t) + g_c\sqrt{N}\beta_{bf}(t)\sin\alpha_f(t) - \dot{\tilde{\beta}}_{af}(t)\sin\alpha_f(t) - \gamma'\tilde{\beta}_{af}(t)\sin\alpha_f(t)]/\sqrt{\rho_{cf}(t)},$$
$$\alpha_f(t) = -\tilde{\delta}t + \delta_2\int_0^t \frac{\tilde{\beta}_{af}^2(t')}{\rho_{cf}(t')}dt', \tag{28}$$

where we have defined $\tilde{\beta}_{af}(t) = ie^{-i\delta_2 t}\beta_{af}(t)$, $\tilde{\beta}_{cf}(t) = e^{-i\tilde{\delta}t}\beta_{cf}(t)$, and $\rho_{cf}(t) = |\tilde{\beta}_{cf}(t)|^2$.

## IV. NUMERICAL INVESTIGATION OF MARKOVIAN AND NON-MARKOVIAN CASES

As the memory effect may be helpful in quantum information processing, the non-Markovian dynamics plays important roles in the description of open systems. Among these topics, the system consisting of $N$ atoms interacting with the multiple environments is of particular interest. Therefore, we wish to derive the dynamics of the system coupled to the multiple environments. Our aim is to control the production of $M$ output single-photon wave packets from the cavity by tuning the driving field. In this section we set $M = 1$, i.e., a single-photon generation in the non-Markovian regime. The output single-photon wave packet needs to satisfy $\beta_b(0) = [\dot{\alpha}_{\text{out}_j}(0) + \lambda_j\alpha_{\text{out}_j}(0)]/\lambda_j\sqrt{\gamma_j} \equiv 0$ and

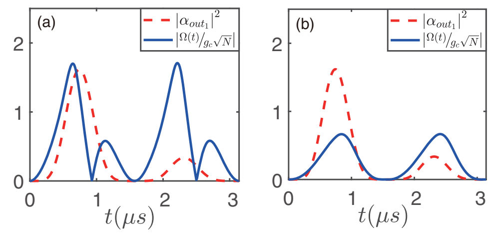


FIG. 2. Generation of the single-photon pulse for the target shape wave packet $\alpha_{\text{out}_1}(t)$. The parameters are $\gamma' = 6\pi$ MHz and $g_c = 30\pi$ MHz [152,153]. The other parameters are $\gamma_1 = 10$ MHz, $\delta_1 = \delta_2 = 0$, $N = 40$, $B_1 = 2$ MHz, and $\Gamma_1 = 0.5$ MHz. The system initially is prepared in state $|c, 0, 0\rangle$. For comparison, $|\Omega(t)/g_c\sqrt{N}|$ (blue solid lines) and $|\alpha_{\text{out}_1}(t)|^2$ (red dashed lines) are plotted, where $\alpha_{\text{out}_1}(t)$ and $\Omega(t)$ are given by Eqs. (29) and (30), respectively. Note that, in this case, we choose (a) $\lambda_1 = 2.31$ MHz (corresponding to the non-Markovian regime) and (b) $\lambda_1 = 30$ MHz (corresponding to the Markovian approximation).

$\dot{\beta}_b(0) = [\ddot{\alpha}_{\text{out}_j}(0) + \lambda_j\dot{\alpha}_{\text{out}_j}(0)]/\lambda_j\sqrt{\gamma_j} \equiv 0$ [originating from Eq. (19) and its derivative in Eq. (10) at $t = 0$ under the initial conditions $\alpha_{\text{in}_j}(t) = 0$, $\beta_b(0) = 0$, $\beta_c(0) = 1$, and $\beta_a(0) = 0$], i.e., three conditions $\alpha_{\text{out}_1}(0) = 0$, $\dot{\alpha}_{\text{out}_1}(0) = 0$, and $\ddot{\alpha}_{\text{out}_1}(0) = 0$, where the output single-photon wave packet is assumed as a real single-photon wave packet (meeting the normalization condition)

$$\alpha_{\text{out}_1}(t) = A_1 e^{-\Gamma_1 t}\sin^3 B_1 t, \tag{29}$$

with the system being initially prepared in $|c, 0, 0\rangle$, corresponding to $\beta_c(0) = 1$ and population of the atom in other states being initially zero. Here $A_1 = 2\sqrt{2(36B_1^6\Gamma_1 + 49B_1^4\Gamma_1^3 + 14B_1^2\Gamma_1^5 + \Gamma_1^7)/3\sqrt{5}B_1^3}$ is the normalization coefficient. In addition, assuming $\delta_1 = \delta_2 = 0$, leading to $Q(t) = 0$ and $\alpha(t) = 0$, we get

$$\Omega(t) = [\dot{\tilde{\beta}}_a(t) - g_c\sqrt{N}\beta_b(t) + \gamma'\tilde{\beta}_a(t)]/\sqrt{\rho_c(t)}. \tag{30}$$

With the output single-photon pulse given by Eq. (29), we assume $B_1 = 2$ MHz and damped rate $\Gamma_1 = 0.5$ MHz shown in Figs. 2(a) and 2(b), which plot $|\alpha_{\text{out}_1}(t)|^2$ and $|\Omega(t)/g_c\sqrt{N}|$ as functions of time $t$. It is found from Fig. 2 that the driving field has different shapes when we control the generation of an output single-photon wave packet in the Markovian and non-Markovian regimes. Next we show that with a driving field, one can manipulate and change the characteristics of the photon generation.

Figure 3 compares the control schemes obtained with and without the Markovian approximations. To be specific, the population of the state $|c\rangle$ in the Markovian approximation is compared with the case without the Markovian approximation as shown in Fig. 3(a), while Fig. 3(c) shows the comparison of the real driving field with and without the Markovian approximations. As shown in Figs. 3(a) and 3(c), the system exhibits non-Markovian dynamics, and we easily see that $\Omega(t)$, $\Omega_f(t)$ and $\rho_c(t)$, $\rho_{cf}(t)$ [the subscript $f$ corresponds to the quantities under the Markovian approximation given by Eq. (27)] have apparent differences, called backflowing phenomena, when the spectral width of the environment is small ($\lambda_1 = 2.31$ MHz), which can be understood by memory effects in the photon emission of the non-Markovian environment. In addition, from Figs. 3(b) and 3(d) we see that the optimal driving field and population of the state $|c\rangle$ in the non-Markovian case for a large spectral width $\lambda_1$ are in good agreement with those in the Markovian approximation. This also confirms that the single-photon wave packets derived with the Markovian approximation have almost the same results as those in the non-Markovian regime when the spectral width $\lambda_1$ equals 30 MHz in Figs. 3(b) and 3(d).

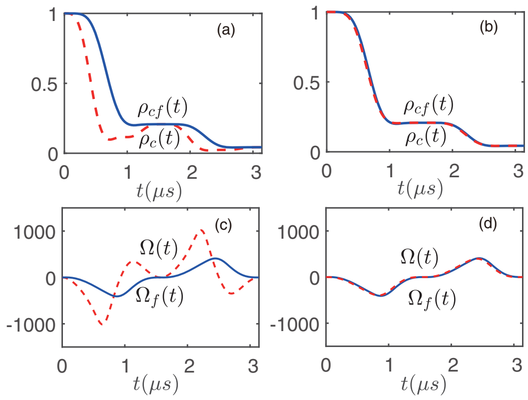


FIG. 3. Populations $\rho_{cf}(t)$ and $\rho_c(t)$ of the state $|c\rangle$ (a) with and (b) without the Markovian approximations are plotted with blue solid and red dashed lines, where $\rho_c(t)$ and $\rho_{cf}(t)$ are given by Eqs. (23) and (27), respectively. The real optimal driving field designed (c) with and (d) without the Markovian approximations, i.e., $\Omega_f(t)$ and $\Omega(t)$, are plotted with blue solid and red dashed lines, where $\Omega(t)$ and $\Omega_f(t)$ are determined by Eqs. (30) and (27), respectively. The parameters are $\gamma_1 = 10$ MHz, $\gamma' = 6\pi$ MHz, $g_c = 30\pi$ MHz, $\delta_1 = \delta_2 = 0$, $N = 40$, $B_1 = 2$ MHz, $\Gamma_1 = 0.5$ MHz, and (a) and (c) $\lambda_1 = 2.31$ MHz and (b) and (d) $\lambda_1 = 30$ MHz.

In order to see the continuous influence of the increase of the spectral width on the single-photon generation, we plot $\rho_c(t)$ and $\rho_{cf}(t)$ as functions of $t$ and $\lambda_1$ in Fig. 4. Figures 4(a) and 4(b) show that the populations of the excited state $\rho_c(t)$ and $\rho_{cf}(t)$ have obvious differences when $\lambda_1$ increases from 2 MHz to 10 MHz. As shown in Figs. 4(c) and 4(d), the Markovian approximation produces almost the same results as the exact case when $\lambda_1$ increases from 10 MHz to 20 MHz. Therefore, Fig. 4 has given the validity range of the Markovian approximation.

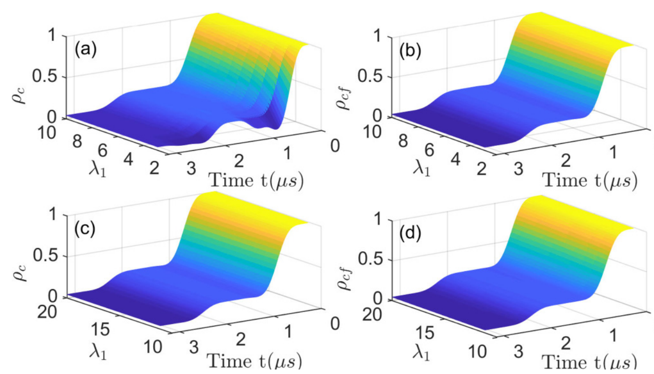


FIG. 4. Evolution of the population of state $|c\rangle$ as a function of $t$ and $\lambda_1$, where $\rho_c(t)$ and $\rho_{cf}(t)$ are given by Eqs. (23) and (27), respectively. The parameters are $\gamma_1 = 10$ MHz, $\gamma' = 6\pi$ MHz, $g_c = 30\pi$ MHz, $\delta_1 = \delta_2 = 0$, $N = 40$, $B_1 = 2$ MHz, and $\Gamma_1 = 0.5$ MHz.

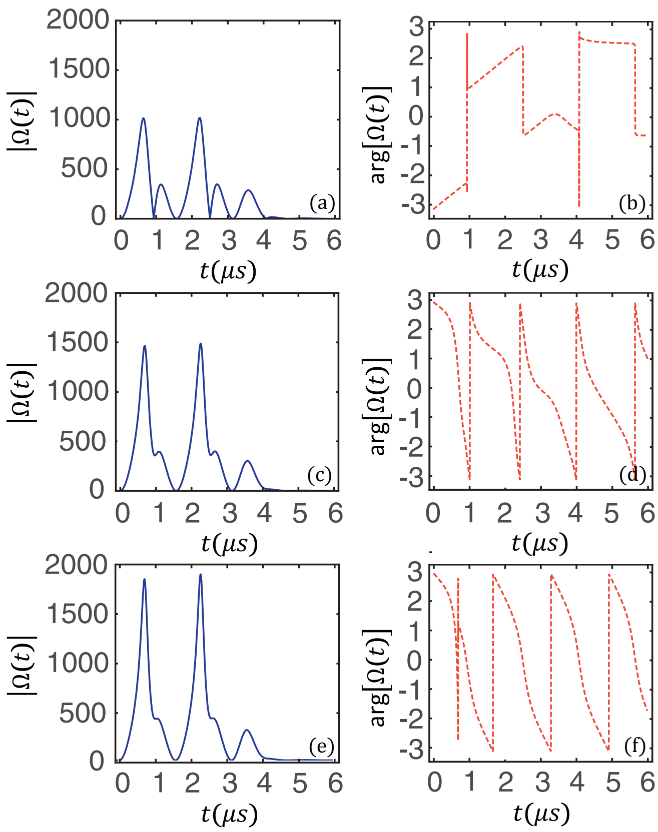


FIG. 5. Influence of the generations of the complex single-photon wave packet $\alpha_{\text{out}_1}(t) = A_1 e^{-\Gamma_1 t}\sin^3(B_1 t)e^{-ic_e t}$ with $A_1 = 2\sqrt{2(36B_1^6\Gamma_1 + 49B_1^4\Gamma_1^3 + 14B_1^2\Gamma_1^5 + \Gamma_1^7)}/3\sqrt{5}B_1^3$ on the modulus and argument for the optimal driving field $\Omega(t)$ in the non-Markovian regime, which can be obtained by Eq. (24). The parameters are $\lambda_1 = 2.31$ MHz, $\delta_1 = 1$ MHz, $\delta_2 = 2$ MHz, $\gamma_1 = 10$ MHz, $\gamma' = 6\pi$ MHz, $g_c = 30\pi$ MHz, $N = 40$, $B_1 = 2$ MHz, $\Gamma_1 = 0.5$ MHz, and (a) and (b) $c_e = 0.01$ MHz, (c) and (d) $c_e = 1.5$ MHz, and (e) and (f) $c_e = 1.9$ MHz.

Before concluding the section we discuss complex single-photon wave packet generations with non-Markovian effects, where the two nonzero detunings $\delta_1 = 1$ MHz and $\delta_2 = 2$ MHz. We assume that the complex single-photon wave packet takes $\alpha_{\text{out}_1}(t) = A_1 e^{-\Gamma_1 t}\sin^3(B_1 t)e^{-ic_e t}$, with $A_1 = 2\sqrt{2(36B_1^6\Gamma_1 + 49B_1^4\Gamma_1^3 + 14B_1^2\Gamma_1^5 + \Gamma_1^7)}/3\sqrt{5}B_1^3$ in Fig. 5, which leads to the modulus and argument for the optimal driving field $\Omega(t)$ generating a single-photon wave packet of arbitrary temporal shape from an optical cavity coupled with $N$ three-level atoms in the non-Markovian regime, which can be obtained by Eq. (24). From Fig. 5 we find that a gradual increase of phase $c_e$ for the complex single-photon wave packet with all the other parameters fixed has a huge impact on the modulus and argument for the optimal driving field.

## V. MULTIPLE NON-MARKOVIAN ENVIRONMENTS INTERACTING WITH THE ONE-SIDED CAVITY

In many realistic scenarios, the quantum system can simultaneously couple with multiple environments [154,155]. In this section we study that the cavity simultaneously interacts with the multiple non-Markovian input-output fields corresponding to Eq. (1). When the first single-photon wave packet generated by the Markovian system is the same as the non-Markovian case, setting all the other spectral widths not equaling the first one will lead to the Markovian system not generating the same multiple single-photon wave packets as the non-Markovian one, while the spectral widths of the different environments taking the same values can generate this. Now we go into the details. To generate the multiple single-photon wave packets from the cavity, assuming $\alpha_{\text{in}_j}(t) = 0$ with Eq. (11), we have $\alpha_{\text{out}_j}(t) = \int_0^t d\tau\, k_j(t-\tau)\beta_b(\tau)$ and

$$
\begin{aligned}
\beta_b(t) &= \frac{\dot{\alpha}_{\text{out}_1}(t) + \lambda_1\alpha_{\text{out}_1}(t)}{\lambda_1\sqrt{\gamma_1}}\\
&\;\;\vdots\\
&= \frac{\dot{\alpha}_{\text{out}_j}(t) + \lambda_j\alpha_{\text{out}_j}(t)}{\lambda_j\sqrt{\gamma_j}}\\
&\;\;\vdots\\
&= \frac{\dot{\alpha}_{\text{out}_m}(t) + \lambda_m\alpha_{\text{out}_m}(t)}{\lambda_m\sqrt{\gamma_m}}\\
&\;\;\vdots\\
&= \frac{\dot{\alpha}_{\text{out}_M}(t) + \lambda_M\alpha_{\text{out}_M}(t)}{\lambda_M\sqrt{\gamma_M}}
\end{aligned}
\tag{31}
$$

for the non-Markovian case, where $j = 1, 2, \ldots, M$ and $m = 1, 2, \ldots, M$. Equation (31) shows that the generated single-photon wave packets are not independent of each other but satisfy certain correlations related to non-Markovian spectral parameters. In particular, the Markovian approximation gives

$$
\begin{aligned}
\beta_{bf}(t) &= \frac{\alpha_{\text{out}_{1f}}(t)}{\sqrt{\gamma_1}} = \cdots = \frac{\alpha_{\text{out}_{jf}}(t)}{\sqrt{\gamma_j}}\\
&= \cdots = \frac{\alpha_{\text{out}_{mf}}(t)}{\sqrt{\gamma_m}} = \cdots = \frac{\alpha_{\text{out}_{Mf}}(t)}{\sqrt{\gamma_M}},
\end{aligned}
\tag{32}
$$

where $\beta_{bf}(t)$ and $\alpha_{\text{out}_{jf}}(t)$ with the subscript $f$ correspond to the quantities under the Markovian approximation.

We discuss the multiple single-photon generations in the Markovian and non-Markovian systems considering the following aspects.

(a) If the cavity only interacts with an input-output field ($M = 1$), the Markovian system can generate the same single-photon wave packet as the non-Markovian one, i.e., $\alpha_{\text{out}_{1f}}(t) = \alpha_{\text{out}_1}(t)$ [the initial conditions $\alpha_{\text{out}_1}(0) = 0$, $\dot{\alpha}_{\text{out}_1}(0) = 0$, and $\ddot{\alpha}_{\text{out}_1}(0) = 0$ need to be satisfied, which can be seen from the first paragraph of Sec. IV], where the optimal driving field $\Omega(t)$ of Eq. (30) falls in the non-Markovian regime, while the optimal driving field $\Omega_f(t)$ under the Markovian approximation is given by Eq. (27).

(b) Under some special conditions, the Markovian system can generate the same (or different) multiple ($M \geqslant 2$) single-photon wave packets as the non-Markovian one. Seven possible situations should be considered, labeled (i)–(vii) below.

We assume that the Markovian system can generate the same single-photon wave packet as the non-Markovian one, e.g.,

$$\alpha_{\text{out}_1}(t) = \alpha_{\text{out}_{1f}}(t) \equiv \sqrt{\frac{\gamma_1}{\gamma_j}}\alpha_{\text{out}_{jf}}(t), \tag{33}$$

where the second identity originates from Eq. (32). Of course, we can also set $\alpha_{\text{out}_1}(t) = \alpha_{\text{out}_{pf}}(t)$ $(p = 2, 3, \ldots, M)$, which is discussed in (v), while (vii) corresponds to the case of generating two of the same single-photon wave packets $\alpha_{\text{out}_{1f}}(t) = \alpha_{\text{out}_1}(t)$ and $\alpha_{\text{out}_{2f}}(t) = \alpha_{\text{out}_2}(t)$ for $M \geqslant 3$. On the contrary, if the Markovian system cannot generate any of the same single-photon wave packets as the non-Markovian one, it is not necessary to establish the relationship between Eqs. (31) and (32).

Substituting Eq. (33) into the first equation of Eq. (31), we get $\beta_b(t) = \dot{\alpha}_{\text{out}_{jf}}(t) + \lambda_1\alpha_{\text{out}_{jf}}(t)/\lambda_1\sqrt{\gamma_j}$, which equals the third equation of Eq. (31); then

$$\frac{\dot{\alpha}_{\text{out}_{jf}}(t) + \lambda_1\alpha_{\text{out}_{jf}}(t)}{\lambda_1\sqrt{\gamma_j}} = \frac{\dot{\alpha}_{\text{out}_m}(t) + \lambda_m\alpha_{\text{out}_m}(t)}{\lambda_m\sqrt{\gamma_m}}. \tag{34}$$

If $m = j$, Eq. (34) is reduced to

$$\frac{\dot{\alpha}_{\text{out}_{jf}}(t)}{\lambda_1} - \frac{\dot{\alpha}_{\text{out}_j}(t)}{\lambda_j} + \alpha_{\text{out}_{jf}}(t) - \alpha_{\text{out}_j}(t) = 0. \tag{35}$$

(i) In the first case, we assume

$$\alpha_{\text{out}_{1f}}(t) = \alpha_{\text{out}_1}(t), \ldots, \alpha_{\text{out}_{jf}}(t) = \alpha_{\text{out}_j}(t), \ldots, \alpha_{\text{out}_{Mf}}(t) = \alpha_{\text{out}_M}(t) \tag{36}$$

and get from Eq. (35)

$$\lambda_1 = \cdots = \lambda_j = \cdots = \lambda_M \equiv \lambda, \tag{37}$$

where the difference between the Markovian and non-Markovian systems is that the optimal driving fields have different forms, i.e., $\Omega(t)$ is determined by Eq. (30), while $\Omega_f(t)$ takes Eq. (27). According to Eq. (32) and normalization condition $\sum_{j=1}^{M}\mu_j = 1$ with $\mu_j = \int dt|\alpha_{\text{out}_{jf}}(t)|^2$, we obtain the relation between $\gamma_j$ and $\mu_j$ as

$$\gamma_j = \frac{\mu_j\gamma_1}{\mu_1}. \tag{38}$$

For the identical output single-photon wave packets, i.e., $\alpha_{\text{out}_{1f}}(t) = \cdots = \alpha_{\text{out}_{jf}}(t) = \cdots = \alpha_{\text{out}_{Mf}}(t)$, we get $\mu_1 = \cdots\mu_j = \cdots = \mu_M = 1/M$.

(ii) However, if all the other spectral widths do not equal the first one, i.e.,

$$\lambda_1 \neq \lambda_2, \ldots, \lambda_1 \neq \lambda_j, \ldots, \lambda_1 \neq \lambda_M, \tag{39}$$

we have

$$\alpha_{\text{out}_2f}(t) \neq \alpha_{\text{out}_2}(t), \ldots, \alpha_{\text{out}_{jf}}(t) \neq \alpha_{\text{out}_j}(t), \ldots, \alpha_{\text{out}_{Mf}}(t) \neq \alpha_{\text{out}_M}(t), \tag{40}$$

which shows that the Markovian system cannot generate the same multiple single-photon wave packets as the non-Markovian one [a single-photon wave packet generated here is assumed to be equal, e.g., $\alpha_{\text{out}_{1f}}(t) = \alpha_{\text{out}_1}(t)$ in Eq. (33)]. In this case, the relations given by Eq. (31) between $\alpha_{\text{out}_j}(t)$ and $\alpha_{\text{out}_1}(t)$ in the non-Markovian regime are determined as

$$\alpha_{\text{out}_j}(t) = \frac{\lambda_j\sqrt{\gamma_j}}{\lambda_1\sqrt{\gamma_1}}\int_0^t dt_1[\dot{\alpha}_{\text{out}_1}(t_1) + \lambda_1\alpha_{\text{out}_1}(t_1)]e^{-\lambda_j(t-t_1)}, \tag{41}$$

which satisfies the normalization condition $\sum_{j=1}^{M}\nu_j = 1$ with

$$\nu_j = \int dt|\alpha_{\text{out}_j}(t)|^2. \tag{42}$$

(iii) As can be seen from Eq. (35), the generated single-photon wave packets can also be partially equal, e.g., $\alpha_{\text{out}_{1f}}(t) = \alpha_{\text{out}_1}(t)$, $\alpha_{\text{out}_{3f}}(t) = \alpha_{\text{out}_3}(t)$, and $\alpha_{\text{out}_{5f}}(t) = \alpha_{\text{out}_5}(t) = \cdots$, with $\lambda_1 = \lambda_3 = \lambda_5 = \cdots$, and $\alpha_{\text{out}_{2f}}(t) \neq \alpha_{\text{out}_2}(t)$, $\alpha_{\text{out}_{4f}}(t) \neq \alpha_{\text{out}_4}(t)$, and $\alpha_{\text{out}_{6f}}(t) \neq \alpha_{\text{out}_6}(t) = \cdots$, with $\lambda_1 \neq \lambda_2$, $\lambda_1 \neq \lambda_4$, $\lambda_1 \neq \lambda_6, \ldots$.

(iv) Assuming $m \neq j$ and $\alpha_{\text{out}_{jf}}(t) = \alpha_{\text{out}_m}(t)$, based on $\alpha_{\text{out}_1}(t) = \alpha_{\text{out}_{1f}}(t)$, Eq. (34) leads to $\lambda_1 = \lambda_m$ and $\gamma_j = \gamma_m$. For $\lambda_1 \neq \lambda_m$ or $\gamma_j \neq \gamma_m$, we have $\alpha_{\text{out}_{jf}}(t) \neq \alpha_{\text{out}_m}(t)$.

(v) If $\alpha_{\text{out}_1}(t) = \alpha_{\text{out}_{pf}}(t)$ $(p = 2, 3, \ldots, M)$, substituting it into Eq. (31), we get $[\dot{\alpha}_{\text{out}_{pf}}(t) + \lambda_1\alpha_{\text{out}_{pf}}(t)]/\lambda_1\sqrt{\gamma_1} = [\dot{\alpha}_{\text{out}_m}(t) + \lambda_m\alpha_{\text{out}_m}(t)]/\lambda_m\sqrt{\gamma_m}$, which gives $\lambda_1 = \lambda_m$ and $\gamma_1 = \gamma_m$ when $\alpha_{\text{out}_{pf}}(t) = \alpha_{\text{out}_m}(t)$. Setting $\lambda_1 \neq \lambda_m$ or $\gamma_1 \neq \gamma_m$, we obtain $\alpha_{\text{out}_{pf}}(t) \neq \alpha_{\text{out}_m}(t)$ when $\alpha_{\text{out}_1}(t) = \alpha_{\text{out}_{pf}}(t)$.

(vi) When the same single-photon wave packet generated by the Markovian and non-Markovian systems in Eq. (33) is not assumed to be $\alpha_{\text{out}_1}(t) = \alpha_{\text{out}_{1f}}(t)$ but $\alpha_{\text{out}_j}(t) = \alpha_{\text{out}_{jf}}(t)$, we have $\lambda_j = \lambda_m$ if $\alpha_{\text{out}_{mf}}(t) = \alpha_{\text{out}_m}(t)$ and then $\alpha_{\text{out}_{mf}}(t) \neq \alpha_{\text{out}_m}(t)$ for $\lambda_j \neq \lambda_m$.

(vii) If the Markovian system can generate two of the same single-photon wave packets $\alpha_{\text{out}_{1f}}(t) = \alpha_{\text{out}_1}(t)$ and $\alpha_{\text{out}_{2f}}(t) = \alpha_{\text{out}_2}(t)$ (leading to $\lambda_1 = \lambda_2$) as the non-Markovian one [corresponding to the case for generating the same single-photon wave packet in Eq. (33)] for $M \geqslant 3$, Eqs. (36) and (37) remain unchanged, while Eqs. (39) and (40) become $\lambda_1 = \lambda_2 \neq \lambda_3, \ldots, \lambda_1 = \lambda_2 \neq \lambda_j, \ldots, \lambda_1 = \lambda_2 \neq \lambda_M$ and $\alpha_{\text{out}_{3f}}(t) \neq \alpha_{\text{out}_3}(t), \ldots, \alpha_{\text{out}_{jf}}(t) \neq \alpha_{\text{out}_j}(t), \ldots, \alpha_{\text{out}_{Mf}}(t) \neq \alpha_{\text{out}_M}(t)$.

From the above discussion, the results in (i)–(vii) can also be obtained from Eqs. (32) and (41), which in particular lead to $\alpha_{\text{out}_j}(t)/\alpha_{\text{out}_1}(t) = \sqrt{\gamma_j/\gamma_1}$ if $\lambda_1 = \lambda_j$ [also derived from $\alpha_{\text{out}_j}(t) = \lambda_j\sqrt{\gamma_j}\int_0^t d\tau\, e^{-\lambda_j(t-\tau)}\beta_b(\tau)$ above Eq. (31)]. Next we are not going to discuss the situations (iii)–(vii) in detail, but mainly focus on the cases (i) and (ii).

### A. Multiple single-photon generations by setting the equal spectral widths for different environments

If the spectral widths of the different environments take the same values in Eq. (37), we show that the system under the Markovian approximation can generate the same single-photon wave packets as the non-Markovian one shown in Figs. 6–9, i.e., $\alpha_{\text{out}_{jf}}(t) = \alpha_{\text{out}_j}(t)$ given by Eq. (36). We consider three types of working mechanisms: (I) The one-sided cavity interacts with one input-output field ($M = 1$ and $\mu_1 = 1$), (II) the one-sided cavity interacts simultaneously with two identical input-output fields ($M = 2$, $\lambda_1 = \lambda_2 \equiv \lambda$, and $\mu_1 = \mu_2 = \frac{1}{2}$), and (III) the one-sided cavity interacts simultaneously with two different input-output fields ($M = 2$, $\lambda_1 = \lambda_2 \equiv \lambda$, $\mu_1 = \frac{1}{3}$, and $\mu_2 = \frac{2}{3}$). We plot the system that

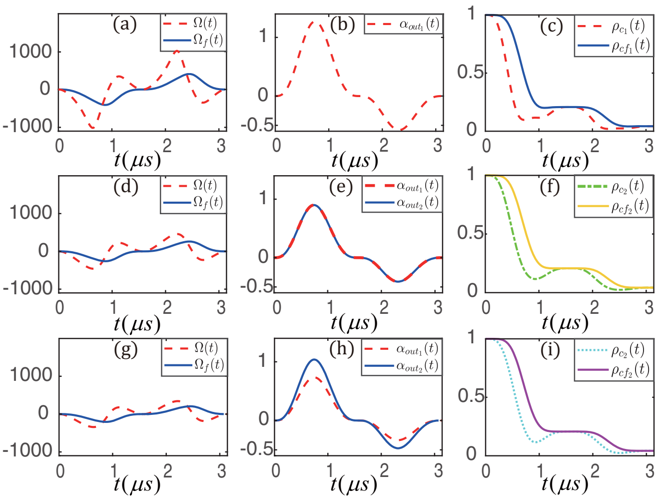


FIG. 6. In order to compare the cavity interacting with one [$\alpha_{\text{out}_1}(t)=A_2e^{-\Gamma_2 t}\sin^3 B_2 t$, where $A_2=2\sqrt{2(36B_2^6\Gamma_2+49B_2^4\Gamma_2^3+14B_2^2\Gamma_2^5+\Gamma_2^7)/3\sqrt{5}B_2^3}$], two identical [$\alpha_{\text{out}_1}(t)=\alpha_{\text{out}_2}(t)=A_3e^{-\Gamma_3 t}\sin^3 B_3 t$, with $A_3=2\sqrt{36B_3^6\Gamma_3+49B_3^4\Gamma_3^3+14B_3^2\Gamma_3^5+\Gamma_3^7/3\sqrt{5}B_3^3}$], and two different input-output fields ($\alpha_{\text{out}_1}(t)=A_4e^{-\Gamma_4 t}\sin^3 B_4 t$ and $\alpha_{\text{out}_2}(t)=\sqrt{\gamma_2/\gamma_1}\int_0^t dt_1[\dot{\alpha}_{\text{out}_1}(t_1)+\lambda\alpha_{\text{out}_1}(t_1)]e^{-\lambda(t-t_1)}$, with $A_4=2\sqrt{2(36B_4^6\Gamma_4+49B_4^4\Gamma_4^3+14B_4^2\Gamma_4^5+\Gamma_4^7)/3\sqrt{15}B_4^3}$) in the Markovian and non-Markovian cases, we plot (a), (d), and (g) the optimal driving field $\Omega_f(t)$ in Eq. (27) and $\Omega(t)$ given by Eq. (30) with and without the Markovian approximations; (b), (e), and (h) output wavepackets; and (c), (f), and (i) population [$\rho_c(t)$ in Eq. (23) and $\rho_{cf}(t)$ in Eq. (27)]. The parameters are $\gamma_1=10$ MHz, $\gamma'=6\pi$ MHz, $g_c=30\pi$ MHz, $\lambda=2.31$ MHz, $\delta_1=\delta_2=0$, $N=40$, $B_2=B_3=B_4=2$ MHz, and $\Gamma_2=\Gamma_3=\Gamma_4=0.5$ MHz.

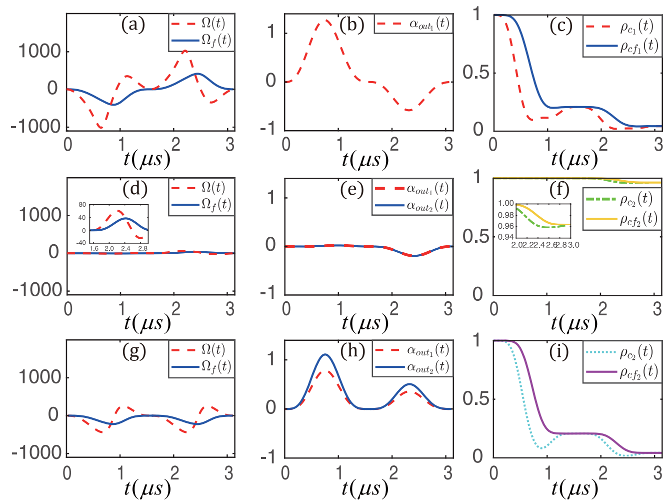


FIG. 8. Three different output single-photon wave packets with non-Markovian effects: (a)–(c) $\alpha_{\text{out}_1}(t)=A_2e^{-\Gamma_2 t}\sin^3 B_2 t$, with $A_2=2\sqrt{2(36B_2^6\Gamma_2+49B_2^4\Gamma_2^3+14B_2^2\Gamma_2^5+\Gamma_2^7)/3\sqrt{5}B_2^3}$; (d)–(f) $\alpha_{\text{out}_1}(t)=\alpha_{\text{out}_2}(t)=A_3t^3e^{-\Gamma_3 t}\sin^3 B_3 t$, with $A_3=2\sqrt{2/45}\sqrt{1/72\Gamma_3^7+\Gamma_3(d_1+d_2+240B_3^4d_3+72B_3^2d_4)/720}$, where $d_1=6/(4B_3^2+\Gamma_3^2)^4-1/(9B_3^2+\Gamma_3^2)^4-15/(B_3^2+\Gamma_3^2)^4$, $d_2=192B_3^6[5/(B_3^2+\Gamma_3^2)^7-128/(4B_3^2+\Gamma_3^2)^7+243/(9B_3^2+\Gamma_3^2)^7]$, $d_3=32/(4B_3^2+\Gamma_3^2)^6-27/(9B_3^2+\Gamma_3^2)^6-5/(B_3^2+\Gamma_3^2)^6$, and $d_4=5/(B_3^2+\Gamma_3^2)^5-8/(4B_3^2+\Gamma_3^2)^5+3/(9B_3^2+\Gamma_3^2)^5$; and (g)–(i) $\alpha_{\text{out}_1}(t)=A_4e^{-\Gamma_4 t}\sin^4 B_4 t$, with $A_4=2\sqrt{576B_4^8\Gamma_4+820B_4^6\Gamma_4^3+273B_4^4\Gamma_4^5+30B_4^2\Gamma_4^7+\Gamma_4^9/z}$, $z=3\sqrt{105}B_4^4$, and $\alpha_{\text{out}_2}(t)=\sqrt{\gamma_2/\gamma_1}\int_0^t dt_1[\dot{\alpha}_{\text{out}_1}(t_1)+\lambda\alpha_{\text{out}_1}(t_1)]e^{-\lambda(t-t_1)}$. In this case, we take $B_2=B_3=B_4=2$ MHz, $\Gamma_2=\Gamma_3=\Gamma_4=0.5$ MHz, and $\lambda=2.31$ MHz. The other parameters and vertical ordinates are given in Fig. 6.

works in three working mechanisms in Fig. 6, which shows the driving field, the output fields, and the population of state $|c\rangle$ in the non-Markovian and Markovian cases with a comparison when the parameter $\lambda$ is fixed to the value 2.31 MHz in three cases. Figures 6(a), 6(d), and 6(g) show that the control driving fields obtained with and without the Markovian approximations are different in three cases. Figures 6(b), 6(e), and 6(h) show the shapes of an output single-photon wave packet, two identical wave packets, and two different wave

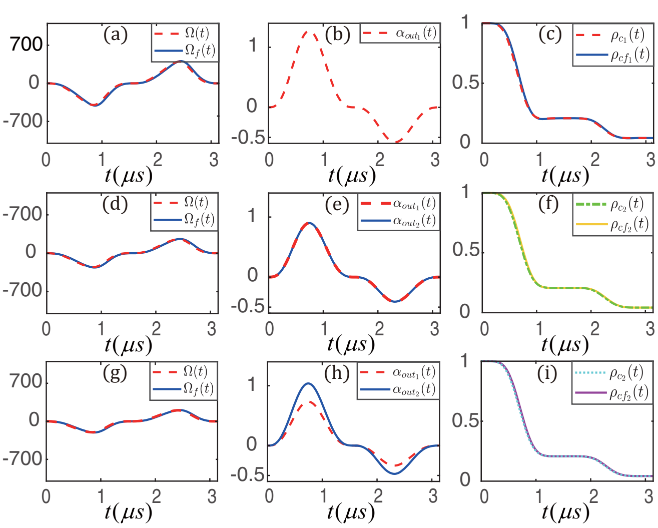


FIG. 7. Case of the Markovian approximation, where the parameters are the same as in Fig. 6 except $\lambda=30$ MHz.

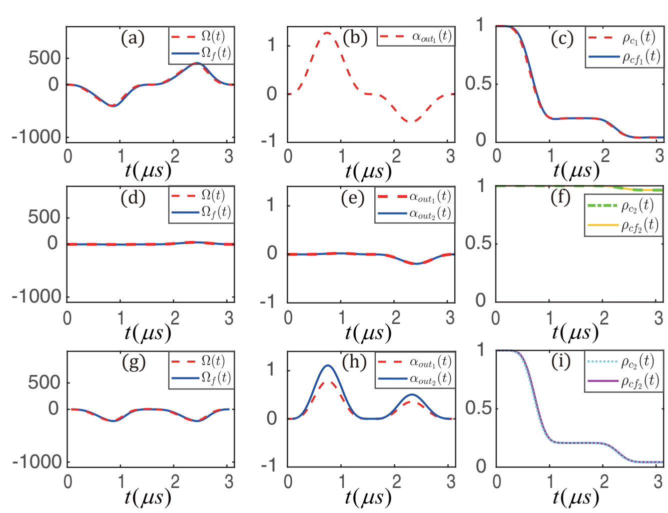


FIG. 9. Case of the Markovian approximation with $\lambda=30$ MHz. The other parameters are the same as in Fig. 8.

packets, respectively. Figures 6(c), 6(f), and 6(i) show the difference of the populations of the state $|c\rangle$ when the system works in three cases. Compared with the Markovian case, we learn that non-Markovianity-caused backflow to the state $|c\rangle$ occurs when the spectral width $\lambda$ is small in three cases.

However, when the spectral width is tuned to $\lambda = 30$ MHz, the results given by the non-Markovian regime are in good agreement with those given in the Markovian approximation. In Figs. 7(a), 7(d), and 7(g) the Markovian approximation produces almost the same driving field results as the exact solution (non-Markovian regime with $\lambda = 30$ MHz). Similarly, the population of the state $|c\rangle$ in the non-Markovian regime controlled by the driving field is consistent with that in the Markovian approximation in three cases when $\lambda = 30$ MHz in Figs. 7(c), 7(f), and 7(i).

As the second concrete example, we take different function forms of output field envelops in Figs. 8 and 9, where the three rows correspond to $\alpha_{\mathrm{out}_1}(t) = A_2 e^{-\Gamma_2 t}\sin^3 B_2 t$, $\alpha_{\mathrm{out}_1}(t) = \alpha_{\mathrm{out}_2}(t) = A_3 t^3 e^{-\Gamma_3 t}\sin^3 B_3 t$, and $\alpha_{\mathrm{out}_1}(t) = A_4 e^{-\Gamma_4 t}\sin^4 B_4 t$ and $\alpha_{\mathrm{out}_2}(t) = \sqrt{\gamma_2/\gamma_1}\int_0^t dt_1[\dot{\alpha}_{\mathrm{out}_1}(t_1) + \lambda\alpha_{\mathrm{out}_1}(t_1)]e^{-\lambda(t-t_1)}$, respectively. The parameters are $B_2 = B_3 = B_4 = 2$ MHz and $\Gamma_2 = \Gamma_3 = \Gamma_4 = 0.5$ MHz. We see that the output field envelopes are obviously different from those of Fig. 6. Similarly, the difference between Figs. 8 and 9 depends on the value of spectral width $\lambda$, where $\lambda = 2.31$ MHz corresponds to the non-Markovian regime, as shown in Fig. 8, while the Markovian approximation is characterized by $\lambda = 30$ MHz in Fig. 9.

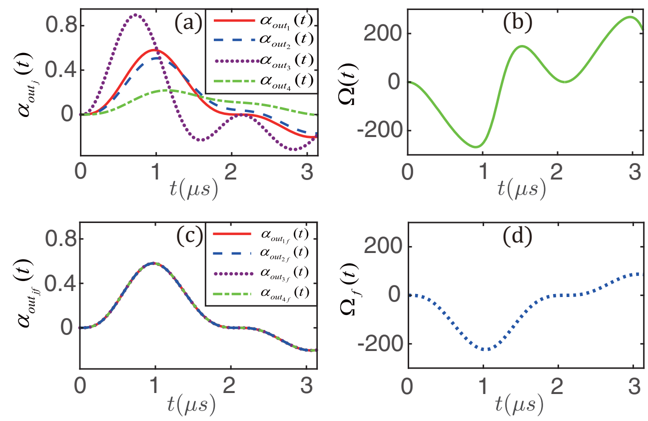


FIG. 10. To generate the multiple ($M = 4$) single-photon wave packets with the normalization factors $\nu_1 = \frac{1}{4}$, $\nu_2 = \frac{1}{5}$, $\nu_3 = \frac{1}{2}$, and $\nu_4 = \frac{1}{20}$, we plot (a) four output single-photon wave packets $\alpha_{\mathrm{out}_1}(t)$, $\alpha_{\mathrm{out}_2}(t)$, $\alpha_{\mathrm{out}_3}(t)$, and $\alpha_{\mathrm{out}_4}(t)$ given by Eq. (43) in the non-Markovian regime, which are separated, and (c) four output single-photon wave packets $\alpha_{\mathrm{out}_{1f}}(t)$, $\alpha_{\mathrm{out}_{2f}}(t)$, $\alpha_{\mathrm{out}_{3f}}(t)$, and $\alpha_{\mathrm{out}_{4f}}(t)$ under the Markovian approximation totally overlapped due to the equal normalization factors $\mu_1 = \mu_2 = \mu_3 = \mu_4 = \frac{1}{4}$ revealed from Eq. (46). The (b) $\Omega(t)$ and (d) $\Omega_f(t)$ are determined by Eqs. (30) and (27), respectively. The other parameters are $\lambda_1 = 2$ MHz, $B = 1.5$ MHz, $\Gamma = 0.5$ MHz, $\gamma_1 = 10$ MHz, $\gamma' = 6\pi$ MHz, $g_c = 30\pi$ MHz, $\delta_1 = \delta_2 = 0$, and $N = 40$. With these parameters, we obtain $\lambda_2 = 1.52$ MHz, $\lambda_3 = 24.87$ MHz, and $\lambda_4 = 0.439$ MHz given by Eq. (45).

### B. Multiple single-photon generations for all other spectral widths not equaling the first one

If the spectral widths satisfy Eq. (39), we take the first output single-photon wave packet as $\alpha_{\mathrm{out}_1}(t) = E_1 e^{-\Gamma t}\sin^3 Bt$ and then obtain $\alpha_{\mathrm{out}_j}(t)$ from Eq. (41) as

$$\alpha_{\mathrm{out}_j}(t) = D_j e^{-\lambda_j t}\left(24B^3\frac{\lambda_1 - \lambda_j}{C_j} + 3h_1^{(j)} - h_3^{(j)}\right), \tag{43}$$

where $D_j = E_1\lambda_j\sqrt{\gamma_j/\gamma_1}/4\lambda_1$, $E_1 = 2\sqrt{2\nu_1(36B^6\Gamma + 49B^4\Gamma^3 + 14B^2\Gamma^5 + \Gamma^7)}/3\sqrt{5}B^3$, $h_n^{(j)} = e^{t(\lambda_j - \Gamma)}\{nB(\lambda_j - \lambda_1)\cos(nBt) + [(nB)^2 + (\Gamma - \lambda_1)(\Gamma - \lambda_j)]\sin(nBt)\}/[(nB)^2 + (\Gamma - \lambda_j)^2]$, and $C_j = [B^2 + (\Gamma - \lambda_j)^2][9B^2 + (\Gamma - \lambda_j)^2]$. Similar to Eq. (38), Eq. (42) gives

$$\gamma_j = \frac{5\nu_j\gamma_1\lambda_1^2[B^2 + (\Gamma + \lambda_j)^2][9B^2 + (\Gamma + \lambda_j)^2]}{\lambda_j\nu_1\left[16\Gamma(4B^2 + \Gamma^2)\lambda_1^2 + a_1\lambda_j + 4\Gamma a_2\lambda_j^2 + a_2\lambda_j^3\right]}, \tag{44}$$

where $a_1 = 5(B^2 + \Gamma^2)(9B^2 + \Gamma^2) + (41B^2 + 29\Gamma^2)\lambda_1^2$ and $a_2 = 9B^2 + \Gamma^2 + 5\lambda_1^2$. We show that the decay rate $\gamma_j$ in Eq. (31) equals $\gamma_j$ given by Eq. (32), together with Eqs. (38) and (44), which lead to $M$ constraint conditions

$$\frac{5\nu_j\mu_1\lambda_1^2}{\mu_j\lambda_j\nu_1} = \frac{16\Gamma(4B^2 + \Gamma^2)\lambda_1^2 + a_1\lambda_j + 4\Gamma a_2\lambda_j^2 + a_2\lambda_j^3}{[B^2 + (\Gamma + \lambda_j)^2][9B^2 + (\Gamma + \lambda_j)^2]}. \tag{45}$$

We show that the equality of different spectral widths is not restricted [e.g., see $\lambda_2 = \lambda_3 = 3.149$ MHz $\neq \lambda_1$ in Fig. 13(a)] as long as they satisfy Eqs. (39) and (45) when all the other parameters are fixed [if $j = 1$, Eq. (45) giving $5\lambda_1 = 5\lambda_1$ is trivial, which results in the fact that Eq. (45) has $M - 1$ effective equations]. Moreover, assuming $\alpha_{\mathrm{out}_{1f}}(t) = \alpha_{\mathrm{out}_1}(t) = E_1 e^{-\Gamma t}\sin^3 Bt$ (i.e., $\nu_1 = \mu_1$), through Eqs. (32) and (38) we obtain the output single-photon wave packet under the Markovian approximation

$$\alpha_{\mathrm{out}_{jf}}(t) = E_1\sqrt{\frac{\gamma_j}{\gamma_1}}e^{-\Gamma t}\sin^3 Bt \equiv E_1\sqrt{\frac{\mu_j}{\mu_1}}e^{-\Gamma t}\sin^3 Bt. \tag{46}$$

We point out that the condition of generating any two equal single-photon wave packets $\alpha_{\mathrm{out}_{jf}}(t)$ and $\alpha_{\mathrm{out}_{mf}}(t)$ under the Markovian approximation is $\mu_j = \mu_m$, as seen from Eq. (46), while the corresponding non-Markovian case for $\alpha_{\mathrm{out}_j}(t) = \alpha_{\mathrm{out}_m}(t)$ requires

$$\lambda_j = \lambda_m, \quad \mu_j = \mu_m, \quad \nu_j = \nu_m, \tag{47}$$

which originate from Eqs. (38), (41), and (42).

When all the other spectral widths do not equal the first one shown in Eq. (39), by setting $M = 4$, we find that four output single-photon wave packets in the non-Markovian regime in Fig. 10(a) are separated, which originates from the normalization factors $\nu_1 = \frac{1}{4}$, $\nu_2 = \frac{1}{5}$, $\nu_3 = \frac{1}{2}$, and $\nu_4 = \frac{1}{20}$ and the spectral widths $\lambda_1 = 2$ MHz, $\lambda_2 = 1.52$ MHz, $\lambda_3 = 24.87$ MHz, and $\lambda_4 = 0.439$ MHz not satisfying Eq. (47). In contrast, the output single-photon wave packets $\alpha_{\mathrm{out}_{1f}}(t)$, $\alpha_{\mathrm{out}_{2f}}(t)$, $\alpha_{\mathrm{out}_{3f}}(t)$, and $\alpha_{\mathrm{out}_{4f}}(t)$ under the Markovian approximation are totally overlapped due to the equal normalization factor $\mu_1 = \mu_2 = \mu_3 = \mu_4 = \frac{1}{4}$ of Eq. (46) in Fig. 10(c). However, in Fig. 11(c) the output single-photon wave

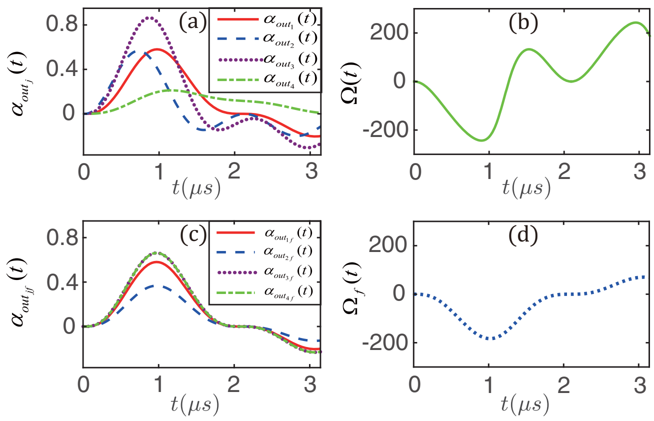


FIG. 11. With the partially nonequal normalization factors $\mu_1 = \frac{1}{4}$, $\mu_2 = \frac{1}{10}$, $\mu_3 = \frac{13}{40}$, and $\mu_4 = \frac{13}{40}$ ($M = 4$), (c) two output single-photon wave packets $\alpha_{\text{out}_{3f}}(t)$ and $\alpha_{\text{out}_{4f}}(t)$ in Eq. (46) under the Markovian approximation are overlapped, while (a) four output single-photon wave packets $\alpha_{\text{out}_1}(t)$, $\alpha_{\text{out}_2}(t)$, $\alpha_{\text{out}_3}(t)$, and $\alpha_{\text{out}_4}(t)$ of Eq. (43) in the non-Markovian regime are separated, where the normalization factors $\nu_1 = \frac{1}{4}$, $\nu_2 = \frac{1}{5}$, $\nu_3 = \frac{1}{2}$, and $\nu_4 = \frac{1}{20}$. The (b) $\Omega(t)$ and (d) $\Omega_f(t)$ are taken from Eqs. (30) and (27), respectively. The other parameters are $\lambda_1 = 2$ MHz, $B = 1.5$ MHz, $\Gamma = 0.5$ MHz, $\gamma_1 = 10$ MHz, $\gamma' = 6\pi$ MHz, $g_c = 30\pi$ MHz, $\delta_1 = \delta_2 = 0$, and $N = 40$, which lead to $\lambda_2 = 24.87$ MHz, $\lambda_3 = 4.3$ MHz, and $\lambda_4 = 0.36$ MHz calculated by Eq. (45).

packets $\alpha_{\text{out}_{3f}}(t)$ and $\alpha_{\text{out}_{4f}}(t)$ under the Markovian approximation in Eq. (46) are overlapped, which differ from those in the non-Markovian regime in Fig. 11(a), where the partially nonequal normalization factors take $\mu_1 = \frac{1}{4}$, $\mu_2 = \frac{1}{10}$, $\mu_3 = \frac{13}{40}$, and $\mu_4 = \frac{13}{40}$. Moreover, the completely nonequal normalization factors $\mu_1 = \frac{1}{4}$, $\mu_2 = \frac{1}{6}$, $\mu_3 = \frac{1}{8}$, and $\mu_4 = \frac{11}{24}$ induce the complete separation of the multiple output single-photon wave packets under the Markovian approximation in Fig. 12(c), but they also have envelops different from those in Fig. 12(a) in the non-Markovian regime. With the selected parameters meeting the condition (47), two single-photon wave packets $\alpha_{\text{out}_2}(t)$ and $\alpha_{\text{out}_3}(t)$ of four single-photon wave packets in the non-Markovian regime are equal and shown in

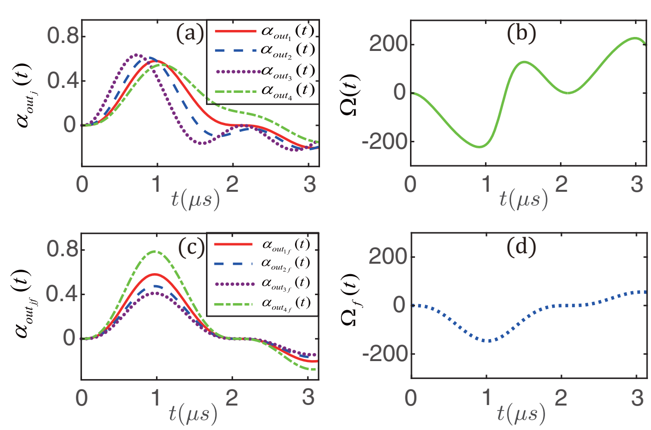


FIG. 12. Completely nonequal normalization factors $\mu_1 = \frac{1}{4}$, $\mu_2 = \frac{1}{6}$, $\mu_3 = \frac{1}{8}$, and $\mu_4 = \frac{11}{24}$ ($M = 4$) lead to (c) four output single-photon wave packets $\alpha_{\text{out}_{1f}}(t)$, $\alpha_{\text{out}_{2f}}(t)$, $\alpha_{\text{out}_{3f}}(t)$, and $\alpha_{\text{out}_{4f}}(t)$ given by Eq. (46) under the Markovian approximation being completely separated and (a) four output single-photon wave packets in the non-Markovian regime given by $\alpha_{\text{out}_1}(t)$, $\alpha_{\text{out}_2}(t)$, $\alpha_{\text{out}_3}(t)$, and $\alpha_{\text{out}_4}(t)$ of Eq. (43). The (b) $\Omega(t)$ and (d) $\Omega_f(t)$ are determined by Eqs. (30) and (27), respectively. The other parameters are $\nu_1 = \nu_2 = \nu_3 = \nu_4 = \frac{1}{4}$, $\lambda_1 = 2$ MHz, $B = 1.5$ MHz, $\Gamma = 0.5$ MHz, $\gamma_1 = 10$ MHz, $\gamma' = 6\pi$ MHz, $g_c = 30\pi$ MHz, $\delta_1 = \delta_2 = 0$, and $N = 40$. With these parameters, Eq. (45) gives $\lambda_2 = 4.047$ MHz, $\lambda_3 = 24.87$ MHz, and $\lambda_4 = 1.028$ MHz.

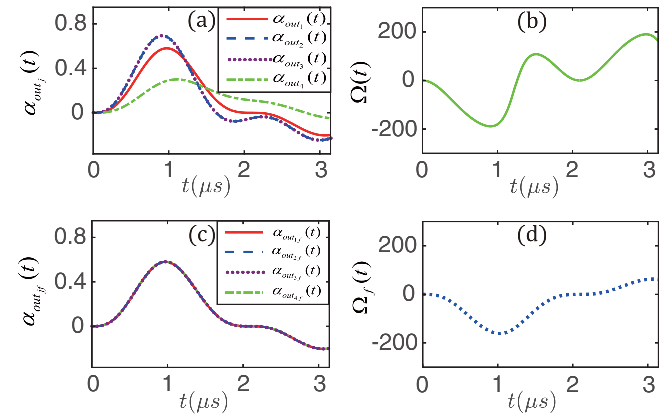


FIG. 13. (a) Two equal single-photon wave packets $\alpha_{\text{out}_2}(t)$ and $\alpha_{\text{out}_3}(t)$ of four single-photon wave packets in the non-Markovian regime are generated, where $\lambda_2 = \lambda_3 = 3.149$ MHz, $\mu_2 = \mu_3 = \frac{1}{4}$, and $\nu_2 = \nu_3 = \frac{1}{3}$ satisfy Eq. (47). (c) Four output single-photon wave packets $\alpha_{\text{out}_{1f}}(t)$, $\alpha_{\text{out}_{2f}}(t)$, $\alpha_{\text{out}_{3f}}(t)$, and $\alpha_{\text{out}_{4f}}(t)$ given by Eq. (46) under the Markovian approximation are totally overlapped. The parameters are $\mu_1 = \mu_4 = \frac{1}{4}$, $\nu_1 = \frac{1}{4}$, $\nu_4 = \frac{1}{12}$, and $\lambda_4 = 0.667$ MHz, from Eq. (45). The other parameters are the same as in Fig. 10.

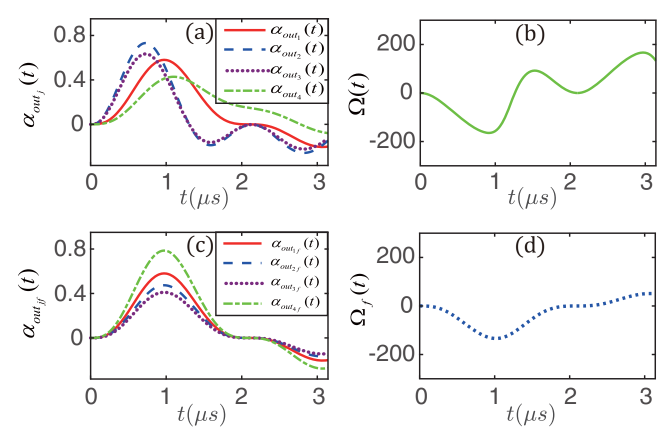


FIG. 14. (a) When the condition in Eq. (47) for generating two equal single-photon wave packets is broken, i.e., $\mu_2 = \frac{1}{6}$, $\mu_3 = \frac{1}{8}$, $\nu_2 = \frac{1}{3}$, and $\nu_3 = \frac{1}{4}$ do not satisfy Eq. (47), the single-photon wave packets $\alpha_{\text{out}_2}(t)$ and $\alpha_{\text{out}_3}(t)$ in the non-Markovian regime are separated compared with Fig. 13(a). (c) In this case, four output single-photon wave packets $\alpha_{\text{out}_{1f}}(t)$, $\alpha_{\text{out}_{2f}}(t)$, $\alpha_{\text{out}_{3f}}(t)$, and $\alpha_{\text{out}_{4f}}(t)$ given by Eq. (46) under the Markovian approximation are completely separated due to the completely nonequal normalization factors. Equation (45) is satisfied by taking the parameters $\mu_1 = \frac{1}{4}$, $\mu_4 = \frac{11}{24}$, $\nu_1 = \frac{1}{4}$, $\nu_4 = \frac{1}{6}$, $\lambda_2 = \lambda_3 = 24.87$ MHz, and $\lambda_4 = 0.717$ MHz. The other parameters are the same as in Fig. 10.

Fig. 13(a), while Fig. 14 shows the case for all single-photon wave packets being separated.

To summarize, if the spectral widths of the different environments take the equal values in Eq. (37), we show that the output single-photon wave packet $\alpha_{\mathrm{out}_j}(t)$ of Eq. (31) in the non-Markovian regime equals $\alpha_{\mathrm{out}_{jf}}(t)$ of Eq. (32) under the Markovian approximation [see Eq. (36)]. However, if all the other spectral widths do not equal the first one in Eq. (39), when the first single-photon wave packet generated by the Markovian system is the same as the non-Markovian case, the same single-photon wave packet $\alpha_{\mathrm{out}_j}(t)$ of Eq. (31) in the non-Markovian regime cannot be generated [see Eq. (40)] by $\alpha_{\mathrm{out}_{jf}}(t)$ of Eq. (32) under the Markovian approximation because $\alpha_{\mathrm{out}_{jf}}(t)$ is independent of the spectral width $\lambda_j$. Moreover, we find that the $j$th output single-photon wave packet $\alpha_{\mathrm{out}_j}(t)$ given by Eq. (41) can be expanded as a power series of the spectral width $\lambda_j$ as

$$\alpha_{\mathrm{out}_j}(t)=\sum_{n=0}^{\infty}\varepsilon_{j,n}(t)\lambda_j^{n+1}, \tag{48}$$

where the time-dependent expansion coefficient $\varepsilon_{j,n}(t)=(-1)^n\sqrt{\gamma_j}/(\lambda_1 n!\sqrt{\gamma_1})\int_0^t(t-t_1)^n[\dot{\alpha}_{\mathrm{out}_1}(t_1)+\lambda_1\alpha_{\mathrm{out}_1}(t_1)]dt_1$ is determined when the first output single-photon wave packet $\alpha_{\mathrm{out}_1}(t)$ and decay rate $\gamma_j$ are given. After fixing $\alpha_{\mathrm{out}_1}(t)$ and $\gamma_j$, the output single-photon wave packet $\alpha_{\mathrm{out}_j}(t)$ can be controlled by tuning the spectral width $\lambda_j$ [in particular, when $j=1$, Eq. (41) or (48) leads to $\alpha_{\mathrm{out}_1}(t)=\alpha_{\mathrm{out}_1}(t)$], which is induced by non-Markovian effects and has no Markovian counterparts. That is to say, the system for the multiple single-photon generations in the framework of all the other spectral widths not equaling the first one in the non-Markovian regime cannot be replaced by the Markovian one, which is the reason we need to consider the non-Markovian system.

Therefore, we point out that the points discussed above may be lost due to making the Markovian approximation when the multiple single-photon wave packets are generated in the non-Markovian system via setting all the other spectral widths not equaling the first one if the first single-photon wave packets generated by the Markovian and non-Markovian systems are equal.

## VI. EXACT SOLUTIONS FOR THE QUANTUM NETWORK DYNAMICS WITH NON-MARKOVIAN EFFECTS

A non-Markovian quantum network [72,154–157] is composed of sending and receiving nodes, where the simplest possible configuration of quantum transmission between two nodes consists of two atoms which are strongly coupled to their respective cavity modes. We consider in Fig. 15 non-Markovian input-output fields coupled to a cavity chain with $P$ cavities, each of which contains a driven identical three-level atom (e.g., cesium atom [152,153]), whose Hamiltonian reads

$$\begin{aligned}\hat{H}=&\sum_{q=1}^{P}\omega_{cav}^{q}\hat{a}_q^{\dagger}\hat{a}_q+\sum_{q=1}^{P}\left(\omega_b^q\sigma_{bb}^{(q)}+\omega_c^q\sigma_{cc}^{(q)}+\omega_a^q\sigma_{aa}^{(q)}\right)+\sum_{q=2}^{P}\sum_{j=1}^{2}\int\omega_{q,j}\hat{b}_{q,j}^{\dagger}(\omega_{q,j})\hat{b}_{q,j}(\omega_{q,j})d\omega_{q,j}+\int\omega_1\hat{b}_1^{\dagger}(\omega_1)\hat{b}_1(\omega_1)d\omega_1\\&+i\sum_{q=2}^{P}\sum_{j=1}^{2}\int d\omega_{q,j}[\hat{a}_q\hat{b}_{q,j}^{\dagger}(\omega_{q,j})v_{q,j}(\omega_{q,j})-\mathrm{H.c.}]+i\int d\omega_1[\hat{a}_1\hat{b}_1(\omega_1)v_1(\omega_1)-\mathrm{H.c.}]\\&+\sum_{q=1}^{P}[\Omega_q(t)e^{-i\omega_L^q t}\hat{\sigma}_{ac}^{(q)}+g_{c,q}\hat{\sigma}_{ab}^{(q)}\hat{a}_q+\mathrm{H.c.}],\end{aligned} \tag{49}$$

where $\hat{a}_q$ is the annihilation operator for the $q$th cavity with frequency $\omega_{\mathrm{cav}}^q$, which couples with two non-Markovian input-output fields by the coupling strength $v_{q,j}$ (with frequency $\omega_{q,j}$) except the first atom-cavity system with $v_1(\omega_1)$; $\omega_b^q$, $\omega_c^q$, and $\omega_a^q$ are the frequencies of the ground-state hyperfine levels $|b\rangle_q$ and $|c\rangle_q$, and the excited state $|a\rangle_q$ for the atom of the $q$th cavity, respectively. State $|b\rangle_q$ is coupled to the intermediate $|c\rangle_q$ by the cavity with the coupling strength $g_{c,q}$, and $|c\rangle_q$ is coupled to $|a\rangle_q$ by the driving field $\Omega_q(t)$. The atom is initially prepared in state $|c\rangle_1$ in the first cavity, while the atoms of the other cavities are all prepared in state $|b\rangle_q$, and cavities and input fields remain in their vacuum states. We control the driving field $\Omega_1(t)$ to generate an output single-photon wave packet from the first cavity. By combining the sending and receiving processes, the transfer of a photon from one node to another can be easily accomplished, where the generated photon leaks out of the first cavity, propagates along the transmission line, enters the optical cavity at the second node, and so on. The cavity is coupled with the electromagnetic continuum outside, forming a photonic channel [62,63]. The state for the first system can be written as $|\Psi(t)\rangle_1=\beta_{b1}(t)|b,1,0\rangle+\beta_{c1}(t)|c,0,0\rangle+\beta_{a1}(t)|a,0,0\rangle+\int d\omega_1\alpha_{\omega_1}(t)|b,0,1_{\omega_1}\rangle$. However, in the $q$th ($q\in[2,P]$) cavity, the state becomes

$$\begin{aligned}|\Psi(t)\rangle_q=&\beta_{bq}(t)|b,1\rangle_q|0_1,0_2\rangle+\beta_{cq}(t)|c,0\rangle_q|0_1,0_2\rangle+\beta_{aq}(t)|a,0\rangle_q|0_1,0_2\rangle+\int d\omega_{q,1}\alpha_{\omega_{q,1}}(t)|b,0\rangle_q|1_{\omega_1},0_2\rangle\\&+\int d\omega_{q,2}\alpha_{\omega_{q,2}}(t)|b,0\rangle_q|0_1,1_{\omega_2}\rangle,\end{aligned} \tag{50}$$

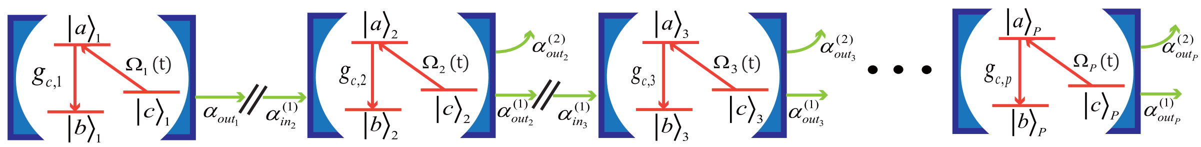

FIG. 15. Illustration of the multiple single-photon generations in driven three-level $\Lambda$ atoms (e.g., cesium atom) coupled to cavities for the non-Markovian quantum network. There are $P$ cavities, where each cavity itself is coupled to the input-output fields forming photonic channels. From the leftmost to rightmost cavities, each contains a driven three-level atom. The coupling parameters and operators defined in the text are indicated. Two cavities are connected by the non-Markovian input-output fields in the following way: The output field of cavity 1 is directed to cavity 2 as its input field and so on.

with the initial conditions $\alpha_{\text{in}_1}=0$, $\beta_{b1}(0)=0$, $\beta_{c1}(0)=1$, and $\beta_{a1}(0)=0$. When the photon producing and receiving processes are completed, we have $\beta_{c1}(t_1)=\dot{\beta}_{c1}(t_1)=0$. If the initial states of the system in the sending and receiving nodes are $|c\rangle_1$ and $|b\rangle_q$ ($q\in[2,P]$), respectively, under the action of the driving field $\Omega_q(t)$ ($q\in[1,P]$), the operation will produce the entangled states in the sending and receiving nodes by

$$\begin{aligned}&|c_1,b_2,b_3\cdots b_P\rangle\otimes|0\rangle\xrightarrow{\Omega_1(t)}\alpha_{\omega_1}|b_1,b_2,b_3\cdots b_P\rangle\otimes\left|\alpha_{\text{out}_1}\right\rangle\xrightarrow{\Omega_2(t)}\alpha_{\omega_{2,1}}|b_1,b_2,b_3\cdots b_P\rangle\otimes\left|\alpha^{(1)}_{\text{out}_2}\right\rangle\\&+\alpha_{\omega_{2,2}}|b_1,b_2,b_3\cdots b_P\rangle\otimes\left|\alpha^{(2)}_{\text{out}_2}\right\rangle\xrightarrow{\Omega_3(t)}\alpha_{\omega_{3,1}}|b_1,b_2,b_3\cdots b_P\rangle\otimes\left|\alpha^{(1)}_{\text{out}_3}\right\rangle+\alpha_{\omega_{3,2}}|b_1,b_2,b_3\cdots b_P\rangle\\&\otimes\left|\alpha^{(2)}_{\text{out}_3}\right\rangle\cdots\xrightarrow{\Omega_P(t)}\alpha_{\omega_{P,1}}|b_1,b_2,a_3\cdots b_P\rangle\otimes\left|\alpha^{(1)}_{\text{out}_P}\right\rangle+\alpha_{\omega_{P,2}}|b_1,b_2,a_3\cdots b_P\rangle\otimes\left|\alpha^{(2)}_{\text{out}_P}\right\rangle,\end{aligned}\tag{51}$$

where $\alpha^{(1)}_{\text{out}_q}(t)=\int d\omega_{q,1}\alpha_{\omega_{q,1}}(t_1)e^{-i\Omega_{q,1}(t-t_1)}/\sqrt{2\pi}$ and $\alpha^{(2)}_{\text{out}_q}(t)=\int d\omega_{q,2}\alpha_{\omega_{q,2}}(t_1)e^{-i\Omega_{q,2}(t-t_1)}/\sqrt{2\pi}$, with $\Omega_{q,j}=\omega_{q,j}-\omega^q_{\text{cav}}$, are the normalized wave packets of the emitted photon. Here $\Omega_q(t)$ denotes the optimal driving field in the $q$th cavity. In our scheme, there are no interactions between two adjacent cavities (the two-sided cavity) [72,155–159], which can be connected by the input and output fields. At the first sending node, there is no incoming photon, i.e., $\alpha_{\text{in}_1}(t)=0$, and we can control the driving field to generate an output single-photon wave packet, where the probability amplitudes for the first cavity in the sending node are determined by

$$\begin{aligned}\dot{\beta}_{b1}(t)&=-ig_{c_1}e^{-i\delta_{2,1}t}\beta_{a1}(t)-\int_0^t d\tau\,\beta_{b1}(\tau)F_{1,1}(t-\tau),\\\dot{\beta}_{c1}(t)&=-i\Omega_1^*(t)e^{-i\delta_{1,1}t}\beta_{a1}(t),\\\dot{\beta}_{a1}(t)&=-ig_{c_1}e^{i\delta_{2,1}t}\beta_{b1}(t)-\gamma_1'\beta_{a1}(t)-i\Omega_1(t)e^{i\delta_{1,1}t}\beta_{c1}(t),\\\alpha_{\text{out}_{1,1}}(t)&=\int_0^t d\tau\,k_{1,1}(t-\tau)\beta_{b1}(\tau),\end{aligned}\tag{52}$$

where $\delta_{1,1}=\omega^1_a-\omega^1_c-\omega^1_L$ and $\delta_{2,1}=\omega^1_a-\omega^1_b-\omega^1_{\text{cav}}$ represent the detunings of the driving field and cavity, respectively, from the atom. Here $F_{1,1}(t)=\int|v_1(\omega_1)|^2e^{-i\Omega_{1,1}t}d\omega_1$ and $k_{1,1}(t)=\int v_1(\omega_1)e^{-i\Omega_{1,1}t}d\omega_1$, with $\Omega_{1,1}=\omega_1-\omega^1_{\text{cav}}$, denote non-Markovian memory and response functions, respectively.

The output field of the first cavity constitutes the input for the second cavity with an appropriate time delay, i.e., $\alpha^{(1)}_{\text{out}_q}(t-\tau)=\alpha^{(1)}_{\text{in}_{q+1}}(t)$, where $\tau$ is a constant related to retardation in the propagation between the mirrors, which is assumed as $\tau=0$ thereafter. The probability amplitudes with the non-Markovian regime for the receiving node of the $q$th ($q\in[2,P]$) cavity are given by

$$\begin{aligned}\dot{\beta}_{bq}(t)&=-ig_{c_q}e^{-i\delta_{2,q}t}\beta_{aq}(t)-\sum_{j=1}^{2}\int_0^t d\tau\,\beta_{bq}(\tau)F_{q,j}(t-\tau)\\&\quad+\sum_{j=1}^{2}\int k^*_{q,j}(t-\tau)\alpha^{(j)}_{\text{in}_q}(\tau)d\tau,\\\dot{\beta}_{cq}(t)&=-i\Omega_q^*(t)e^{-i\delta_{1,q}t}\beta_{aq}(t),\\\dot{\beta}_{aq}(t)&=-ig_{c_q}e^{i\delta_{2,q}t}\beta_{bq}(t)-i\Omega_q(t)e^{i\delta_{1,q}t}\beta_{cq}(t)-\gamma_q'\beta_{aq}(t),\end{aligned}\tag{53}$$

where $\delta_{1,q}=\omega^q_a-\omega^q_c-\omega^q_L$, $\delta_{2,q}=\omega^q_a-\omega^q_b-\omega^q_{\text{cav}}$, $F_{q,j}(t)=\int|v_{q,j}(\omega_{q,j})|^2e^{-i\Omega_{q,j}t}d\omega_{q,j}$, and $k_{q,j}(t)=\int v_{q,j}(\omega_{q,j})e^{-i\Omega_{q,j}t}d\omega_{q,j}$. The non-Markovian input-output relations can be written as

$$\begin{aligned}\alpha^{(1)}_{\text{out}_q}(t)-\alpha^{(1)}_{\text{in}_q}(t)&=\int_0^t d\tau\,k_{q,1}(t-\tau)\beta_{bq}(\tau),\\\alpha^{(2)}_{\text{out}_q}(t)&=\int_0^t d\tau\,k_{q,2}(t-\tau)\beta_{bq}(\tau),\\\alpha^{(1)}_{\text{out}_q}(t)&=\alpha^{(1)}_{\text{in}_{q+1}}(t),\end{aligned}\tag{54}$$

where $\alpha^{(1)}_{\text{out}_1}(t)\equiv\alpha_{\text{out}_1}(t)$. In the past, people in general focused on the sending and receiving processes between two cavities [62,63]. Our scheme can happen between multiple cavities, where each cavity has two input and output fields except the first cavity, where the process of sending and receiving will be repeated all the time. To get the desired wave packets form or state, we can choose which cavity to end the process. The presented results involving an arbitrary number of driven atom-cavity might offer a way to better understand single-photon generation for non-Markovian quantum networks.

## VII. CONCLUSION

In summary, we have studied a general control scheme of a quantum system consisting of $N$ driven three-level atoms coupled to a one-sided cavity interacting with multiple non-Markovian input-output fields. Regarding atoms, there are backflows in the population on the state $|c\rangle$ in the non-Markovian regime, while there are no backflows in the Markovian case. Moreover, we calculated the optimal driving field needed to produce arbitrarily shaped multiple complex single-photon wave packets from the cavity in the non-Markovian case, which depends on two detunings of the cavity and driving field with respect to the three-level atoms. Setting all the other spectral widths not equaling the first one results in the Markovian system not being able to generate the same multiple single-photon wave packets as the non-Markovian one when the first single-photon wave packet generated by the Markovian system is the same as the non-Markovian case, while taking the equal spectral width values for the different environments can generate this. The scheme analyzes specifically the exact results of the cavity interacting simultaneously with the multiple environments in the non-Markovian regime, where the generated different single-photon wave packets satisfy certain connections with the spectral parameters. We showed that a transition occurs from non-Markovian to Markovian regimes by controlling the spectral widths of the environments. Finally, we discussed the dynamics of quantum network consisting of many cavities containing driven three-level atoms for non-Markovian input-output fields.

The studies of non-Markovian multiple single-photon generations in driven three-level atoms coupled to cavity might offer a way to better understand the multiple single-photon generations in quantum network and quantum communications. As an outlook, it will be interesting to explore multiple single-photon generation for the total excitation number nonconserving systems beyond rotating-wave approximations, e.g., isotropic non-rotating-wave interactions $\Omega(t)\hat{\sigma}_{ac}+\Omega^*(t)\hat{\sigma}_{ca}+g(\hat{\sigma}_{ab}+\hat{\sigma}_{ba})(\hat{a}+\hat{a}^\dagger)$ [160,161] plus $\sum_k v_k(\hat{a}+\hat{a}^\dagger)(\hat{b}_k+\hat{b}_k^\dagger)$ [162,163] for the case of an atom, anisotropic nonrotating wave quantum systems $\sum_k[\alpha_k(\hat{S}^\dagger\hat{b}_k+\hat{S}\hat{b}_k^\dagger)+\beta_k(\hat{S}\hat{b}_k+\hat{S}^\dagger\hat{b}_k^\dagger)]$ with $\hat{S}=\hat{\sigma}_{ba}$ or $\hat{a}$ [164–170], and many-body systems [171–176], which are worthy of future investigation.

## ACKNOWLEDGMENTS

H.Z.S. would like to thank Dr. Jia-Xin Yang for valuable discussions. This work was supported by National Natural Science Foundation of China under Grants No. 12175033, No. 12274064, and No. 12147206; National Key R&D Program of China (Grant No. 2021YFE0193500); and Natural Science Foundation of Jilin Province (subject arrangement project) under Grant No. 20210101406JC.

## APPENDIX A: DERIVATION OF EQ. (1)

The total system is composed of a cavity coupled to $N$ three-level atoms driven by a driving field, where the cavity interacts with $M$ non-Markovian input-output fields in Fig. 1, whose Hamiltonian is given by $\hat{H}'=\hat{H}_1+\hat{H}_2$, with

$$\begin{aligned}\hat{H}_1&=\omega_{\rm cav}\hat{a}^\dagger\hat{a}+\sum_{m=1}^{N}\left(\omega_a\hat{\sigma}_{aa}^{(m)}+\omega_b\hat{\sigma}_{bb}^{(m)}+\omega_c\hat{\sigma}_{cc}^{(m)}-i\gamma'\hat{\sigma}_{aa}^{(m)}\right),\\ \hat{H}_2&=\sum_{j=1}^{M}\int\omega_j\hat{b}_j^\dagger(\omega_j)\hat{b}_j(\omega_j)d\omega_j\\ &\quad+\sum_{m=1}^{N}\left[\Omega(t)e^{-i\omega_L t}\hat{\sigma}_{ac}^{(m)}+g_c\hat{a}\hat{\sigma}_{ab}^{(m)}+\text{H.c.}\right]\\ &\quad+i\sum_{j=1}^{M}\int d\omega_j[\nu_j(\omega_j)\hat{a}\hat{b}_j^\dagger(\omega_j)-\text{H.c.}].\end{aligned}\tag{A1}$$

In a rotating frame defined by $\hat{U}=\exp[-i\hat{H}_1t-i\omega_{\rm cav}t\sum_{j=1}^{M}\int\hat{b}_j^\dagger(\omega_j)\hat{b}_j(\omega_j)d\omega_j]$ with $e^{i\omega\hat{a}^\dagger\hat{a}t}\hat{a}e^{-i\omega\hat{a}^\dagger\hat{a}t}=\hat{a}e^{-i\omega t}$ and $e^{i\omega\hat{\sigma}_{aa}t}\hat{\sigma}_{ac}e^{-i\omega\hat{\sigma}_{aa}t}=\hat{\sigma}_{ac}e^{i\omega t}$, we obtain $\hat{H}=\hat{U}^\dagger\hat{H}'\hat{U}-i\hat{U}^\dagger\dot{\hat{U}}\equiv\hat{H}_S+\hat{H}_B+\hat{V}$ in Eq. (1).

## APPENDIX B: DERIVATION OF EQ. (15)

Substituting Eq. (8) into Eq. (4), we have

$$\begin{aligned}\dot{\beta}_b(t)&=-ig_c^*\sqrt{N}e^{-i\delta_2 t}\beta_a(t)\\ &\quad-\sum_{j=1}^{M}\int_{-\infty}^{\infty}\nu_j^*(\omega_j)\alpha_{\omega_j}(0)e^{-i\Omega_{\omega_j}t}d\omega_j\\ &\quad-\sum_{j=1}^{M}\int_0^t\int_{-\infty}^{\infty}|\nu_j(\omega_j)|^2e^{-i\Omega_{\omega_j}(t-\tau)}\beta_b(\tau)d\omega_jd\tau.\end{aligned}\tag{B1}$$

The first equation of Eq. (10) can be derived by substituting Eqs. (12)–(15) into Eq. (B1).

## APPENDIX C: DERIVATION OF EQ. (11)

When $t_1\to t$, with Eqs. (12) and (13), we obtain

$$\begin{aligned}\alpha_{\text{in}_j}(t)+\alpha_{\text{out}_j}(t)&=-\frac{1}{\sqrt{2\pi}}\int_{-\infty}^{\infty}\alpha_{\omega_j}(0)e^{-i\Omega_{\omega_j}t}d\omega_j\\ &\quad+\frac{1}{\sqrt{2\pi}}\int_{-\infty}^{\infty}\alpha_{\omega_j}(t)d\omega_j.\end{aligned}\tag{C1}$$

Substituting Eq. (8) into Eq. (C1) results in

$$\begin{aligned}\alpha_{\text{in}_j}(t)+\alpha_{\text{out}_j}(t)&=\frac{1}{\sqrt{2\pi}}\int_{-\infty}^{\infty}\nu_j(\omega_j)\int_0^t\beta_b(\tau)\\ &\quad\times e^{-i\Omega_{\omega_j}(t-\tau)}d\tau\,d\omega_j,\end{aligned}\tag{C2}$$

which leads to Eq. (11) by substituting Eq. (14) into Eq. (C2).

[1] J. I. Cirac, A. K. Ekert, S. F. Huelga, and C. Macchiavello, Distributed quantum computation over noisy channels, Phys. Rev. A **59**, 4249 (1999).

[2] D. P. DiVincenzo, The physical implementation of quantum computation, Fortschr. Phys. **48**, 771 (2000).

[3] Y. L. Zhou, Y. M. Wang, L. M. Liang, and C. Z. Li, Quantum state transfer between distant nodes of a quantum network via adiabatic passage, Phys. Rev. A **79**, 044304 (2009).

[4] S. J. van Enk, J. I. Cirac, and P. Zoller, Ideal Quantum Communication over Noisy Channels: A Quantum Optical Implementation, Phys. Rev. Lett. **78**, 4293 (1997).

[5] S. Clark, A. Peng, M. Gu, and S. Parkins, Unconditional Preparation of Entanglement between Atoms in Cascaded Optical Cavities, Phys. Rev. Lett. **91**, 177901 (2003).

[6] F. Y. Hong and S. J. Xiong, Quantum communication in a network with serious imperfections, Phys. Rev. A **76**, 052302 (2007).

[7] J. I. Cirac, P. Zoller, H. J. Kimble, and H. Mabuchi, Quantum State Transfer and Entanglement Distribution among Distant Nodes in a Quantum Network, Phys. Rev. Lett. **78**, 3221 (1997).

[8] L. B. Chen, M. Y. Ye, G. W. Lin, Q. H. Du, and X. M. Lin, Generation of entanglement via adiabatic passage, Phys. Rev. A **76**, 062304 (2007).

[9] F. K. Nohama and J. A. Roversi, Two-qubit state transfer between trapped ions using electromagnetic cavities coupled by an optical fibre, J. Phys. B **41**, 045503 (2008).

[10] J. Cho, D. G. Angelakis, and S. Bose, Heralded generation of entanglement with coupled cavities, Phys. Rev. A **78**, 022323 (2008).

[11] A. Gogyan and Y. Malakyan, Deterministic quantum state transfer between remote atoms with photon-number superposition states, Phys. Rev. A **98**, 052304 (2018).

[12] A. Peng and A. S. Parkins, Motion-light parametric amplifier and entanglement distributor, Phys. Rev. A **65**, 062323 (2002).

[13] M. Fleischhauer, S. F. Yelin, and M. D. Lukin, How to trap photons? Storing single-photon quantum states in collective atomic excitations, Opt. Commun. **179**, 395 (2000).

[14] M. D. Lukin, S. F. Yelin, and M. Fleischhauer, Entanglement of Atomic Ensembles by Trapping Correlated Photon States, Phys. Rev. Lett. **84**, 4232 (2000).

[15] M. Fleischhauer and M. D. Lukin, Quantum memory for photons: Dark-state polaritons, Phys. Rev. A **65**, 022314 (2002).

[16] F. Mei, M. Feng, Y. F. Yu, and Z. M. Zhang, Scalable quantum information processing with atomic ensembles and flying photons, Phys. Rev. A **80**, 042319 (2009).

[17] Y. F. Xiao, X. B. Zou, Y. Hu, Z. F. Han, and G. C. Guo, Preparation of microwave single-photon states via a superconducting circuit, Phys. Rev. A **74**, 032309 (2006).

[18] E. Knill, R. Laflamme, and G. J. Milburn, A scheme for efficient quantum computation with linear optics, Nature (London) **409**, 46 (2001).

[19] D. D. M. Welakuh and A. M. Dikandé, Storage and retrieval of time-entangled soliton trains in a three-level atom system coupled to an optical cavity, Opt. Commun. **403**, 27 (2017).

[20] B. Sun, M. S. Chapman, and L. You, Atom-photon entanglement generation and distribution, Phys. Rev. A **69**, 042316 (2004).

[21] S. Brattke, B. T. H. Varcoe, and H. Walther, Generation of Photon Number States on Demand via Cavity Quantum Electrodynamics, Phys. Rev. Lett. **86**, 3534 (2001).

[22] F. L. Semião, R. J. Missori, and K. Furuya, Unconditional Bell-type state generation for spatially separate trapped ions, J. Phys. B **40**, S221 (2007).

[23] W. X. Lai, H. C. Li, and R. C. Yang, Controlled optical switching based on dipole-induced transparency in a cavity-waveguide system, Opt. Commun. **281**, 4048 (2008).

[24] Y. F. Xiao, J. Gao, X. B. Zou, J. F. McMillan, X. Yang, Y. L. Chen, Z. F. Han, G. C. Guo, and C. W. Wong, Coupled quantum electrodynamics in photonic crystal cavities towards controlled phase gate operations, New J. Phys. **10**, 123013 (2008).

[25] S. J. van Enk, H. J. Kimble, and H. Mabuchi, Quantum information processing in cavity-QED, Quantum Inf. Process. **3**, 75 (2004).

[26] C. Y. Hu and J. G. Rarity, Extended linear regime of cavity-QED enhanced optical circular birefringence induced by a charged quantum dot, Phys. Rev. B **91**, 075304 (2015).

[27] J. H. Li, R. Yu, and X. X. Yang, Design of electro-optic switching via a photonic crystal cavity coupled to a quantum-dot molecule and waveguides, Phys. Lett. A **374**, 3762 (2010).

[28] Z. J. Deng, L. M. Liang, J. M. Chen, and C. W. Wu, State transfer and entanglement with atomic ensembles in a one-dimensional fibre-coupled cavity chain, J. Phys. B **43**, 065506 (2010).

[29] S. Xu, H. Z. Shen, and X. X. Yi, Single-photon transistor based on tunable coupling in a cavity quantum electrodynamics system, J. Opt. Soc. Am. B **33**, 1600 (2016).

[30] P. T. Fong and C. K. Law, Bound state in the continuum by spatially separated ensembles of atoms in a coupled-cavity array, Phys. Rev. A **96**, 023842 (2017).

[31] A. Reiserer and G. Rempe, Cavity-based quantum networks with single atoms and optical photons, Rev. Mod. Phys. **87**, 1379 (2015).

[32] H. L. Ma, C. G. Ye, D. Wei, and J. Zhang, Coherence Phenomena in the Phase-Sensitive Optical Parametric Amplification inside a Cavity, Phys. Rev. Lett. **95**, 233601 (2005).

[33] Y. Meng, F. Mei, G. Chen, and S. T. Jia, Topological quantum walks in cavity-based quantum networks, Quantum Inf. Process. **19**, 118 (2020).

[34] C. G. Ye and J. Zhang, Absorptive and dispersive properties in the phase-sensitive optical parametric amplification inside a cavity, Phys. Rev. A **73**, 023818 (2006).

[35] Y. Wang, C. Li, E. M. Sampuli, J. Song, Y. Y. Jiang, and Y. Xia, Enhancement of coherent dipole coupling between two atoms via squeezing a cavity mode, Phys. Rev. A **99**, 023833 (2019).

[36] S. Schmidt and J. Koch, Circuit QED lattices: Towards quantum simulation with superconducting circuits, Ann. Phys. (Berlin) **525**, 395 (2013).

[37] S. I. Schmid and J. Evers, Microcavities coupled to multilevel atoms, Phys. Rev. A **84**, 053822 (2011).

[38] R. Yu, J. H. Li, M. Liu, C. L. Ding, and X. X. Yang, Optical transmission gratings by one driven three-level atom and a microtoroidal resonator, Opt. Commun. **284**, 5263 (2011).

[39] J. Cho and H. W. Lee, Controlled unitary operation between two distant atoms, Phys. Rev. A **72**, 052309 (2005).

[40] H. P. Specht, C. Nölleke, A. Reiserer, M. Uphoff, E. Figueroa, S. Ritter, and G. Rempe, A single-atom quantum memory, Nature (London) **473**, 190 (2011).

[41] M. Mücke, E. Figueroa, J. Bochmann, C. Hahn, K. Murr, S. Ritter, C. J. Villas-Boas, and G. Rempe, Electromagnetically induced transparency with single atoms in a cavity, Nature (London) **465**, 755 (2010).

[42] J. Dilley, P. Nisbet-Jones, B. W. Shore, and A. Kuhn, Single-photon absorption in coupled atom-cavity systems, Phys. Rev. A **85**, 023834 (2012); G. S. Vasilev, D. Ljunggren, and A. Kuhn, Single photons made-to-measure, New J. Phys. **12**, 063024 (2010).

[43] L. Y. Wang, K. Di, Y. F. Zhu, and G. S. Agarwal, Interference control of perfect photon absorption in cavity quantum electrodynamics, Phys. Rev. A **95**, 013841 (2017).

[44] H. Z. Shen, M. Qin, and X. X. Yi, Single-photon storing in coupled non-Markovian atom-cavity system, Phys. Rev. A **88**, 033835 (2013).

[45] G. S. Agarwal, K. Di, L. Y. Wang, and Y. F. Zhu, Perfect photon absorption in the nonlinear regime of cavity quantum electrodynamics, Phys. Rev. A **93**, 063805 (2016).

[46] M. J. Akram, F. Ghafoor, and F. Saif, Electromagnetically induced transparency and tunable Fano resonances in hybrid optomechanics, J. Phys. B **48**, 065502 (2015).

[47] R. R. Oliveira, H. S. Borges, J. A. Souza, and C. J. Villas-Boas, A multitasking device based on electromagnetically induced transparency in optical cavities, Quantum Inf. Process. **17**, 311 (2018).

[48] R. B. Liu, W. Yao, and L. J. Sham, Quantum computing by optical control of electron spins, Adv. Phys. **59**, 703 (2010).

[49] M. Keller, B. Lange, K. Hayasaka, W. Lange, and H. Walther, Continuous generation of single photons with controlled waveform in an ion-trap cavity system, Nature (London) **431**, 1075 (2004).

[50] A. D. Manukhova, K. S. Tikhonov, T. Y. Golubeva, and Y. M. Golubev, Noiseless signal shaping and cluster-state generation with a quantum memory cell, Phys. Rev. A **96**, 023851 (2017).

[51] H. Goto, S. Mizukami, Y. Tokunaga, and T. Aoki, Figure of merit for single-photon generation based on cavity quantum electrodynamics, Phys. Rev. A **99**, 053843 (2019).

[52] H. S. Borges and C. J. Villas-Bôas, Quantum PHASE gate based on electromagnetically induced transparency in optical cavities, Phys. Rev. A **94**, 052337 (2016).

[53] H. Thyrrestrup, A. Hartsuiker, J. M. Gérard, and W. L. Vos, Non-exponential spontaneous emission dynamics for emitters in a time-dependent optical cavity, Opt. Express **21**, 23130 (2013).

[54] E. M. Graefe, A. A. Mailybaev, and N. Moiseyev, Breakdown of adiabatic transfer of light in waveguides in the presence of absorption, Phys. Rev. A **88**, 033842 (2013).

[55] H. S. Borges, D. Z. Rossatto, F. S. Luiz, and C. J. Villas-Boas, Heralded entangling quantum gate via cavity-assisted photon scattering, Phys. Rev. A **97**, 013828 (2018).

[56] N. G. Veselkova, N. I. Masalaeva, and I. V. Sokolov, Cavity-assisted atomic Raman memories beyond the bad cavity limit: Effect of four-wave mixing, Phys. Rev. A **99**, 013814 (2019).

[57] T. Macha, E. Uruñuela, W. Alt, M. Ammenwerth, D. Pandey, H. Pfeifer, and D. Meschede, Nonadiabatic storage of short light pulses in an atom-cavity system, Phys. Rev. A **101**, 053406 (2020).

[58] M. Cai, Y. Q. Lu, M. Xiao, and K. Y. Xia, Optimizing single-photon generation and storage with machine learning, Phys. Rev. A **104**, 053707 (2021).

[59] A. Holleczek, O. Barter, A. Rubenok, J. Dilley, P. B. R. Nisbet-Jones, G. Langfahl-Klabes, G. D. Marshall, C. Sparrow, J. L. O'Brien, K. Poulios, A. Kuhn, and J. C. F. Matthews, Quantum Logic with Cavity Photons From Single Atoms, Phys. Rev. Lett. **117**, 023602 (2016).

[60] O. Morin, M. Körber, S. Langenfeld, and G. Rempe, Deterministic Shaping and Reshaping of Single-Photon Temporal Wave Functions, Phys. Rev. Lett. **123**, 133602 (2019).

[61] N. V. Vitanov, A. A. Rangelov, B. W. Shore, and K. Bergmann, Stimulated Raman adiabatic passage in physics, chemistry, and beyond, Rev. Mod. Phys. **89**, 015006 (2017).

[62] W. Yao, R. B. Liu, and L. J. Sham, Theory of Control of the Spin-Photon Interface for Quantum Networks, Phys. Rev. Lett. **95**, 030504 (2005).

[63] W. Yao, R. B. Liu, and L. J. Sham, Theory of control of the dynamics of the interface between stationary and flying qubits, J. Opt. B **7**, S318 (2005).

[64] Z. Q. Yin, W. L. Yang, L. Sun, and L. M. Duan, Quantum network of superconducting qubits through an optomechanical interface, Phys. Rev. A **91**, 012333 (2015); L. M. Duan, A. Kuzmich, and H. J. Kimble, Cavity QED and quantum-information processing with "hot" trapped atoms, *ibid.* **67**, 032305 (2003).

[65] F. Y. Hong, J. L. Fu, Y. Wu, and Z. Y. Zhu, Room-temperature spin-photon interface for quantum networks, Quantum Inf. Process. **16**, 43 (2017).

[66] F. Y. Hong, Y. Xiang, J. L. Fu, and Z. Y. Zhu, All-electrical control of the photon-charge-qubit interfaces for quantum networks, J. Phys. Soc. Jpn. **81**, 104001 (2012).

[67] J. G. Li, J. Zou, and B. Shao, Non-Markovianity of the damped Jaynes-Cummings model with detuning, Phys. Rev. A **81**, 062124 (2010); J. L. Li, H. Z. Shen, and X. X. Yi, Quantum battery in non-Markovian reservoirs, Opt. Lett. **47**, 5614 (2022); H. Z. Shen, S. Xu, Hong Li, S. L. Wu, and X. X. Yi, Linear response theory for periodically driven systems with non-Markovian effects, *ibid.* **43**, 2852 (2018).

[68] C. W. Gardiner and P. Zoller, *Quantum Noise* (Springer, Berlin, 2000).

[69] H. Z. Shen, S. Xu, Y. H. Zhou, and X. X. Yi, System susceptibility and bound-states in structured reservoirs, Opt. Express **27**, 31504 (2019); R. L. Franco, B. Bellomo, S. Maniscalco, and G. Compagno, Dynamics of quantum correlations in two-qubit systems within non-Markovian environments, Int. J. Mod. Phys. B **27**, 1345053 (2013).

[70] F. Caruso, V. Giovannetti, C. Lupo, and S. Mancini, Quantum channels and memory effects, Rev. Mod. Phys. **86**, 1203 (2014).

[71] F. Y. Hong, Y. Xiang, Z. Y. Zhu, L. Z. Jiang, and L. N. Wu, Robust quantum random access memory, Phys. Rev. A **86**, 010306(R) (2012).

[72] J. Zhang, Y. X. Liu, R. B. Wu, K. Jacobs, and F. Nori, Non-Markovian quantum input-output networks, Phys. Rev. A **87**, 032117 (2013).

[73] H. P. Breuer and F. Petruccione, *The Theory of Open Quantum Systems* (Oxford University Press, Oxford, 2002).

[74] H. N. Xiong, W. M. Zhang, M. W. Y. Tu, and D. Braun, Dynamically stabilized decoherence-free states in

non-Markovian open fermionic systems, Phys. Rev. A **86**, 032107 (2012).
[75] H. Z. Shen, D. X. Li, S. L. Su, Y. H. Zhou, and X. X. Yi, Exact non-Markovian dynamics of qubits coupled to two interacting environments, Phys. Rev. A **96**, 033805 (2017).
[76] T. Yu, L. Diósi, N. Gisin, and W. T. Strunz, Non-Markovian quantum-state diffusion: Perturbation approach, Phys. Rev. A **60**, 91 (1999).
[77] M. W. Jack, M. J. Collett, and D. F. Walls, Non-Markovian quantum trajectories for spectral detection, Phys. Rev. A **59**, 2306 (1999).
[78] C. Cohen-Tannoudji and S. Reynaud, Dressed-atom description of resonance fluorescence and absorption spectra of a multi-level atom in an intense laser beam, J. Phys. B **10**, 345 (1977); Modification of resonance Raman scattering in very intense laser fields, **10**, 365 (1977); Simultaneous saturation of two atomic transitions sharing a common level, **10**, 2311 (1977).
[79] R. Zhang, T. Chen, and X. B. Wang, Deterministic quantum controlled-PHASE gates based on non-Markovian environments, New J. Phys. **19**, 123001 (2017).
[80] H. Z. Shen, S. L. Su, Y. H. Zhou, and X. X. Yi, Non-Markovian quantum Brownian motion in one dimension in electric fields, Phys. Rev. A **97**, 042121 (2018).
[81] H. Z. Shen, S. Xu, H. T. Cui, and X. X. Yi, Non-Markovian dynamics of a system of two-level atoms coupled to a structured environment, Phys. Rev. A **99**, 032101 (2019).
[82] Z. X. Man, Y. J. Xia, and R. Lo Franco, Harnessing non-Markovian quantum memory by environmental coupling, Phys. Rev. A **92**, 012315 (2015); H. Z. Shen, D. X. Li, and X. X. Yi, Non-Markovian linear response theory for quantum open systems and its applications, Phys. Rev. E **95**, 012156 (2017).
[83] M. J. Hartmann, F. G. S. L. Brandão, and M. B. Plenio, Strongly interacting polaritons in coupled arrays of cavities, Nat. Phys. **2**, 849 (2006).
[84] T. Pellizzari, Quantum Networking with Optical Fibres, Phys. Rev. Lett. **79**, 5242 (1997).
[85] A. Biswas and D. A. Lidar, Robust transmission of non-Gaussian entanglement over optical fibers, Phys. Rev. A **74**, 062303 (2006).
[86] Q. A. Turchette, C. J. Myatt, B. E. King, C. A. Sackett, D. Kielpinski, W. M. Itano, C. Monroe, and D. J. Wineland, Decoherence and decay of motional quantum states of a trapped atom coupled to engineered reservoirs, Phys. Rev. A **62**, 053807 (2000).
[87] C. J. Myatt, B. E. King, Q. A. Turchette, C. A. Sackett, D. Kielpinski, W. M. Itano, C. Monroe, and D. J. Wineland, Decoherence of quantum superpositions through coupling to engineered reservoirs, Nature (London) **403**, 269 (2000).
[88] S. Maniscalco, J. Piilo, F. Intravaia, F. Petruccione, and A. Messina, Simulating quantum Brownian motion with single trapped ions, Phys. Rev. A **69**, 052101 (2004).
[89] M. Bayindir, B. Temelkuran, and E. Ozbay, Tight-Binding Description of the Coupled Defect Modes in Three-Dimensional Photonic Crystals, Phys. Rev. Lett. **84**, 2140 (2000).
[90] N. Stefanou and A. Modinos, Impurity bands in photonic insulators, Phys. Rev. B **57**, 12127 (1998).
[91] Y. Xu, Y. Li, R. K. Lee, and A. Yariv, Scattering-theory analysis of waveguide-resonator coupling, Phys. Rev. E **62**, 7389 (2000).
[92] L. L. Lin, Z. Y. Li, and B. Lin, Engineering waveguide-cavity resonant side coupling in a dynamically tunable ultracompact photonic crystal filter, Phys. Rev. B **72**, 165330 (2005).
[93] K. W. Chang and C. K. Law, Non-Markovian master equation for a damped oscillator with time-varying parameters, Phys. Rev. A **81**, 052105 (2010).
[94] H. T. Tan and W. M. Zhang, Non-Markovian dynamics of an open quantum system with initial system-reservoir correlations: A nanocavity coupled to a coupled-resonator optical waveguide, Phys. Rev. A **83**, 032102 (2011).
[95] S. Longhi, Non-Markovian decay and lasing condition in an optical microcavity coupled to a structured reservoir, Phys. Rev. A **74**, 063826 (2006); H. Z. Shen, M. Qin, X. Q. Shao, and X. X. Yi, General response formula and application to topological insulator in quantum open system, Phys. Rev. E **92**, 052122 (2015).
[96] S. B. Xue, R. B. Wu, W. M. Zhang, J. Zhang, C. W. Li, and T. J. Tarn, Decoherence suppression via non-Markovian coherent feedback control, Phys. Rev. A **86**, 052304 (2012).
[97] H. P. Breuer, E. M. Laine, J. Piilo, and B. Vacchini, *Colloquium*: Non-Markovian dynamics in open quantum systems, Rev. Mod. Phys. **88**, 021002 (2016).
[98] H. P. Breuer, E. M. Laine, and J. Piilo, Measure for the Degree of Non-Markovian Behavior of Quantum Processes in Open Systems, Phys. Rev. Lett. **103**, 210401 (2009).
[99] E. M. Laine, J. Piilo, and H. P. Breuer, Measure for the non-Markovianity of quantum processes, Phys. Rev. A **81**, 062115 (2010).
[100] S. Wißmann, A. Karlsson, E. M. Laine, J. Piilo, and H. P. Breuer, Optimal state pairs for non-Markovian quantum dynamics, Phys. Rev. A **86**, 062108 (2012).
[101] S. Lorenzo, F. Plastina, and M. Paternostro, Geometrical characterization of non-Markovianity, Phys. Rev. A **88**, 020102(R) (2013).
[102] Á. Rivas, S. F. Huelga, and M. B. Plenio, Entanglement and Non-Markovianity of Quantum Evolutions, Phys. Rev. Lett. **105**, 050403 (2010).
[103] H. Z. Shen, S. Xu, S. Yi, and X. X. Yi, Controllable dissipation of a qubit coupled to an engineering reservoir, Phys. Rev. A **98**, 062106 (2018).
[104] M. M. Wolf, J. Eisert, T. S. Cubitt, and J. I. Cirac, Assessing Non-Markovian Quantum Dynamics, Phys. Rev. Lett. **101**, 150402 (2008).
[105] X. M. Lu, X. G. Wang, and C. P. Sun, Quantum Fisher information flow and non-Markovian processes of open systems, Phys. Rev. A **82**, 042103 (2010).
[106] D. Chruściński and S. Maniscalco, Degree of Non-Markovianity of Quantum Evolution, Phys. Rev. Lett. **112**, 120404 (2014).
[107] F. Y. Hong and S. J. Xiong, Single-photon transistor using microtoroidal resonators, Phys. Rev. A **78**, 013812 (2008).
[108] Y. F. Xiao, Z. F. Han, and G. C. Guo, Quantum computation without strict strong coupling on a silicon chip, Phys. Rev. A **73**, 052324 (2006).
[109] B. Wang and L. M. Duan, Implementation scheme of controlled SWAP gates for quantum fingerprinting and photonic quantum computation, Phys. Rev. A **75**, 050304(R) (2007).

[110] F. Y. Hong, L. Chen, J. L. Fu, and Z. Y. Zhu, Quantum state transfer between remote nanomechanical qubits, Eur. Phys. J. D **69**, 122 (2015).
[111] E. M. Laine, J. Piilo, and H. P. Breuer, Witness for initial system-environment correlations in open-system dynamics, Europhys. Lett. **92**, 60010 (2010).
[112] J. Dajka and J. Łuczka, Distance growth of quantum states due to initial system-environment correlations, Phys. Rev. A **82**, 012341 (2010).
[113] A. Smirne, H. P. Breuer, J. Piilo, and B. Vacchini, Initial correlations in open-systems dynamics: The Jaynes-Cummings model, Phys. Rev. A **82**, 062114 (2010).
[114] Z. X. Man, A. Smirne, Y. J. Xia, and B. Vacchini, Quantum interference induced by initial system-environment correlations, Phys. Lett. A **376**, 2477 (2012).
[115] C. F. Li, J. S. Tang, Y. L. Li, and G. C. Guo, Experimentally witnessing the initial correlation between an open quantum system and its environment, Phys. Rev. A **83**, 064102 (2011).
[116] I. de Vega and D. Alonso, Dynamics of non-Markovian open quantum systems, Rev. Mod. Phys. **89**, 015001 (2017).
[117] F. Verstraete, M. M. Wolf, and J. I. Cirac, Quantum computation and quantum-state engineering driven by dissipation, Nat. Phys. **5**, 633 (2009).
[118] M. J. Kastoryano, M. M. Wolf, and J. Eisert, Precisely Timing Dissipative Quantum Information Processing, Phys. Rev. Lett. **110**, 110501 (2013).
[119] S. C. Hou, S. L. Liang, and X. X. Yi, Non-Markovianity and memory effects in quantum open systems, Phys. Rev. A **91**, 012109 (2015).
[120] H. Z. Shen, X. Q. Shao, G. C. Wang, X. L. Zhao, and X. X. Yi, Quantum phase transition in a coupled two-level system embedded in anisotropic three-dimensional photonic crystals, Phys. Rev. E **93**, 012107 (2016).
[121] D. Chruściński and A. Kossakowski, Non-Markovian Quantum Dynamics: Local versus Nonlocal, Phys. Rev. Lett. **104**, 070406 (2010).
[122] L. Xin, S. Xu, X. X. Yi, and H. Z. Shen, Tunable non-Markovian dynamics with a three-level atom mediated by the classical laser in a semi-infinite photonic waveguide, Phys. Rev. A **105**, 053706 (2022).
[123] A. W. Chin, S. F. Huelga, and M. B. Plenio, Quantum Metrology in Non-Markovian Environments, Phys. Rev. Lett. **109**, 233601 (2012).
[124] S. Deffner and E. Lutz, Quantum Speed Limit for Non-Markovian Dynamics, Phys. Rev. Lett. **111**, 010402 (2013).
[125] A. J. Leggett, S. Chakravarty, A. T. Dorsey, M. P. A. Fisher, A. Garg, and W. Zwerger, Dynamics of the dissipative two-state system, Rev. Mod. Phys. **59**, 1 (1987).
[126] U. Weiss, *Quantum Dissipative Systems*, 3rd ed. (World Scientific, Singapore, 2008).
[127] S. Gröblacher, A. Trubarov, N. Prigge, G. D. Cole, M. Aspelmeyer, and J. Eisert, Observation of non-Markovian micromechanical Brownian motion, Nat. Commun. **6**, 7606 (2015).
[128] B. H. Liu, L. Li, Y. F. Huang, C. F. Li, G. C. Guo, E. M. Laine, H. P. Breuer, and J. Piilo, Experimental control of the transition from Markovian to non-Markovian dynamics of open quantum systems, Nat. Phys. **7**, 931 (2011).
[129] U. Hoeppe, C. Wolff, J. Küchenmeister, J. Niegemann, M. Drescher, H. Benner, and K. Busch, Direct Observation of Non-Markovian Radiation Dynamics in 3D Bulk Photonic Crystals, Phys. Rev. Lett. **108**, 043603 (2012).
[130] S. J. Xiong, Q. W. Hu, Z. Sun, L. Yu, Q. P. Su, J. M. Liu, and C. P. Yang, Non-Markovianity in experimentally simulated quantum channels: Role of counterrotating-wave terms, Phys. Rev. A **100**, 032101 (2019).
[131] J. S. Xu, C. F. Li, C. J. Zhang, X. Y. Xu, Y. S. Zhang, and G. C. Guo, Experimental investigation of the non-Markovian dynamics of classical and quantum correlations, Phys. Rev. A **82**, 042328 (2010).
[132] K. H. Madsen, S. Ates, T. Lund-Hansen, A. Löffler, S. Reitzenstein, A. Forchel, and P. Lodahl, Observation of Non-Markovian Dynamics of a Single Quantum Dot in a Micropillar Cavity, Phys. Rev. Lett. **106**, 233601 (2011).
[133] A. Orieux, A. D'Arrigo, G. Ferranti, R. Lo Franco, G. Benenti, E. Paladino, G. Falci, F. Sciarrino, and P. Mataloni, Experimental on-demand recovery of entanglement by local operations within non-Markovian dynamics, Sci. Rep. **5**, 8575 (2015).
[134] A. Smirne, D. Brivio, S. Cialdi, B. Vacchini, and M. G. A. Paris, Experimental investigation of initial system-environment correlations via trace-distance evolution, Phys. Rev. A **84**, 032112 (2011).
[135] R. Hanson, V. V. Dobrovitski, A. E. Feiguin, O. Gywat, and D. D. Awschalom, Coherent dynamics of a single spin interacting with an adjustable spin bath, Science **320**, 352 (2008).
[136] R. Hanson, L. P. Kouwenhoven, J. R. Petta, S. Tarucha, and L. M. K. Vandersypen, Spins in few-electron quantum dots, Rev. Mod. Phys. **79**, 1217 (2007).
[137] J. J. Pla, K. Y. Tan, J. P. Dehollain, W. H. Lim, J. J. L. Morton, D. N. Jamieson, A. S. Dzurak, and A. Morello, A single-atom electron spin qubit in silicon, Nature (London) **489**, 541 (2012).
[138] Z. X. Man, N. B. An, and Y. J. Xia, Non-Markovianity of a two-level system transversally coupled to multiple bosonic reservoirs, Phys. Rev. A **90**, 062104 (2014).
[139] A. Z. Chaudhry and J. B. Gong, Decoherence induced by a composite environment, Phys. Rev. A **89**, 014104 (2014).
[140] C. K. Chan, G. D. Lin, S. F. Yelin, and M. D. Lukin, Quantum interference between independent reservoirs in open quantum systems, Phys. Rev. A **89**, 042117 (2014).
[141] T. J. G. Apollaro, S. Lorenzo, C. Di Franco, F. Plastina, and M. Paternostro, Competition between memory-keeping and memory-erasing decoherence channels, Phys. Rev. A **90**, 012310 (2014).
[142] T. Ma, Y. Chen, T. Chen, S. R. Hedemann, and T. Yu, Crossover between non-Markovian and Markovian dynamics induced by a hierarchical environment, Phys. Rev. A **90**, 042108 (2014).
[143] A. Fruchtman, B. W. Lovett, S. C. Benjamin, and E. M. Gauger, Quantum dynamics in a tiered non-Markovian environment, New J. Phys. **17**, 023063 (2015).
[144] E. Waks and J. Vuckovic, Dipole Induced Transparency in Drop-Filter Cavity-Waveguide Systems, Phys. Rev. Lett. **96**, 153601 (2006).
[145] A. Auffèves-Garnier, C. Simon, J. M. Gérard, and J. P. Poizat, Giant optical nonlinearity induced by a single two-level system interacting with a cavity in the Purcell regime, Phys. Rev. A **75**, 053823 (2007).

[146] T. B. Propp and S. J. van Enk, Quantum networks for single photon detection, Phys. Rev. A **100**, 033836 (2019).

[147] C. W. Gardiner and M. J. Collett, Input and output in damped quantum systems: Quantum stochastic differential equations and the master equation, Phys. Rev. A **31**, 3761 (1985).

[148] D. F. Walls and G. J. Milburn, *Quantum Optics*, 2nd ed. (Springer, Berlin, 2008).

[149] R. M. Rajapakse, T. Bragdon, A. M. Rey, T. Calarco, and S. F. Yelin, Single-photon nonlinearities using arrays of cold polar molecules, Phys. Rev. A **80**, 013810 (2009).

[150] Z. X. Xu, Y. L. Wu, H. L. Liu, S. J. Li, and H. Wang, Fast manipulation of spin-wave excitations in an atomic ensemble, Phys. Rev. A **88**, 013423 (2013).

[151] M. O. Scully and M. S. Zubairy, *Quantum Optics* (Cambridge University Press, Cambridge, 1997).

[152] J. McKeever, A. Boca, A. D. Boozer, R. Miller, J. R. Buck, A. Kuzmich, and H. J. Kimble, Deterministic generation of single photons from one atom trapped in a cavity, Science **303**, 1992 (2004).

[153] J. McKeever, A. Boca, A. D. Boozer, J. R. Buck, and H. J. Kimble, Experimental realization of a one-atom laser in the regime of strong coupling, Nature (London) **425**, 268 (2003).

[154] J. Combes, J. Kerckhoff, and M. Sarovar, The SLH framework for modeling quantum input-output networks, Adv. Phys. X **2**, 784 (2017).

[155] J. Zhang, Y. X. Liu, R. B. Wu, K. Jacobs, S. K. Ozdemir, L. Yang, T. J. Tarn, and F. Nori, Nonlinear quantum input-output analysis using Volterra series, arXiv:1407.8108.

[156] J. Zhang, Y. X. Liu, R. B. Wu, K. Jacobs, and F. Nori, Quantum feedback: Theory, experiments, and applications, Phys. Rep. **679**, 1 (2017).

[157] Y. L. Liu, Z. P. Liu, J. Zhang, and Y. X. Liu, Coherent-feedback-induced photon blockade and optical bistability by an optomechanical controller, arXiv:1407.3036.

[158] M. F. Yanik and S. Fan, Stopping Light All Optically, Phys. Rev. Lett. **92**, 083901 (2004).

[159] M. F. Yanik and S. Fan, Stopping and storing light coherently, Phys. Rev. A **71**, 013803 (2005).

[160] T. Shi, Y. Chang, and J. J. García-Ripoll, Ultrastrong Coupling Few-Photon Scattering Theory, Phys. Rev. Lett. **120**, 153602 (2018).

[161] L. Z. Lo and C. K. Law, Quantum radiation from a shaken two-level atom in vacuum, Phys. Rev. A **98**, 063807 (2018).

[162] H. Z. Shen, Q. Wang, and X. X. Yi, Dispersive readout with non-Markovian environments, Phys. Rev. A **105**, 023707 (2022).

[163] H. Z. Shen, C. Shang, Y. H. Zhou, and X. X. Yi, Unconventional single-photon blockade in non-Markovian systems, Phys. Rev. A **98**, 023856 (2018); H. Z. Shen, Q. Wang, J. Wang, and X. X. Yi, Nonreciprocal unconventional photon blockade in a driven dissipative cavity with parametric amplification, *ibid.* **101**, 013826 (2020).

[164] Q.-T. Xie, S. Cui, J.-P. Cao, L. Amico, and H. Fan, Anisotropic Rabi model, Phys. Rev. X **4**, 021046 (2014).

[165] X.-Y. Chen, L. Duan, D. Braak, and Q.-H. Chen, Multiple ground-state instabilities in the anisotropic quantum Rabi model, Phys. Rev. A **103**, 043708 (2021).

[166] M. A. Rodríguez, P. Tempesta, and P. Winternitz, Reduction of superintegrable systems: The anisotropic harmonic oscillator, Phys. Rev. E **78**, 046608 (2008).

[167] S. Nakajima, Perturbation theory in statistical mechanics, Adv. Phys. **4**, 363 (1955).

[168] Q. Ai, Y. Li, H. Zheng, and C. P. Sun, Quantum anti-Zeno effect without rotating wave approximation, Phys. Rev. A **81**, 042116 (2010).

[169] H. Zheng, Dynamics of a two-level system coupled to ohmic bath: A perturbation approach, Eur. Phys. J. B **38**, 559 (2004); H. Fröhlich, Interaction of electrons with lattice vibrations, Proc. R. Soc. London Ser. A **215**, 291 (1952); Theory of the superconducting state. I. The ground state at the absolute zero of temperature, Phys. Rev. **79**, 845 (1950).

[170] Z. G. Lü and H. Zheng, Quantum dynamics of the dissipative two-state system coupled with a sub-Ohmic bath, Phys. Rev. B **75**, 054302 (2007).

[171] M. H. Fischer, M. Maksymenko, and E. Altman, Dynamics of a Many-Body-Localized System Coupled to a Bath, Phys. Rev. Lett. **116**, 160401 (2016).

[172] V. R. Overbeck and H. Weimer, Time evolution of open quantum many-body systems, Phys. Rev. A **93**, 012106 (2016).

[173] M. V. Medvedyeva, T. Prosen, and M. Žnidarič, Influence of dephasing on many-body localization, Phys. Rev. B **93**, 094205 (2016).

[174] M. Metcalf, J. E. Moussa, W. A. de Jong, and M. Sarovar, Engineered thermalization and cooling of quantum many-body systems, Phys. Rev. Res. **2**, 023214 (2020).

[175] X. S. Xu, J. Thingna, C. Guo, and D. Poletti, Many-body open quantum systems beyond Lindblad master equations, Phys. Rev. A **99**, 012106 (2019).

[176] J. Lebreuilly, A. Biella, F. Storme, D. Rossini, R. Fazio, C. Ciuti, and I. Carusotto, Stabilizing strongly correlated photon fluids with non-Markovian reservoirs, Phys. Rev. A **96**, 033828 (2017).